

## Assessment of A Novel Combined Power and Refrigeration Cycle Using Solar Heat Source Based On the First and Second Laws of Thermodynamics

Hadi Ghaebi<sup>a,\*</sup>, Mohammad Ebadollahi<sup>b</sup>, Majid Amidpour<sup>b</sup>

<sup>a</sup>Department of Mechanical Engineering, Faculty of Engineering, University of Mohaghegh Ardabili, P.O. Box 179, Ardabil, Iran

<sup>b</sup>Faculty of Mechanical Engineering, Department of Energy System Engineering, K.N. Toosi University of Technology, Pardis Ave., Tehran, Iran

Received: 11-07-2022

Accepted: 04-12-2022

### Abstract

The present study proposes modified solar-driven combined power and ejector refrigeration cycles (CPERCs) for low-temperature heat sources. The proposed cycles are constructed from a combination of simple organic Rankine cycle (ORC), ORC with an internal heat exchanger (IHE), a regenerative ORC, and a regenerative ORC with an IHE, with an ejector refrigeration cycle (ERC). The ejector is driven by the exhausts from the turbine to produce more power and refrigeration, simultaneously. The three modified ORCs are introduced to improve the performance of the energy systems. The first and second laws of thermodynamics have been applied to each cycle using R245fa and isobutene as working fluids. Also, solar energy is utilized as the main heat source of the energy system. Concerning each proposed cycle, the thermodynamic model has been validated by previous works. Using isobutene as a working fluid, the maximum thermal and exergetic efficiencies have been obtained at 50.46 and 58.08 %, respectively, which corresponded to regenerative combined power and ejector refrigeration cycle with an IHE. In general, the thermal efficiency of a system is improved by 7.54 and 5.76 % through this state-of-art modification using R245fa and isobutene as working fluids, respectively. This demonstrated that isobutene can be a good candidate for CPERCs based on the first and second laws of thermodynamics. Throughout these modifications, cooling capacity and net produced power of cycles are also increased, successively. In all proposed cycles, the generator has the highest exergy destruction ratio, falling into the range of (29.82-34.73) and (22.9-25.93) kW for R245fa and isobutene, respectively.

**Keywords:** Modified combined power and ejector refrigeration cycles (MCPERCs); Organic Rankine cycles (ORCs); Ejector refrigeration cycle; Low-temperature heat sources

DOI: 10.22059/jsr.2022.345700.1249 DOR: 20.1001.1.25883097.2023.8.1.6.2

### 1. Introduction

In recent years with a rapid increase in the cost of energy consumption, solar energy has received considerable attention from different industrial and residential applicants all around the world [1]. Among all well-known solar-driven devices, an

ejector can be used instead of conventional compressor to consume much less power for refrigeration purposes. Ejectors due to their simple structure, cost-effectiveness, operation condition, and most importantly, running by low-grade sources, can be attributed in many different arenas such as simultaneous power and refrigeration production industry. On the other hand, natural energy resources

\*Corresponding Author Email Address: [hghaebi@uma.ac.ir](mailto:hghaebi@uma.ac.ir)

are being depleted, and utilization of renewable energy seems the only way to save posterity [2, 3]. Based on the sustainable and green aspects of solar energy, exploiting this source has been raised in recent years [4, 5]. Sustainable economic condition motivates the government to invest in renewable energy projects [6, 7]. solar energy has been used in combined power generation set-ups such as Kalina cycle (KC), organic Rankine cycle (ORC), and absorption power systems (APS) [8, 9].

Solar resource has been utilized as motivation energy in electricity, cooling, and heating systems as well as CHP and multigeneration systems [10-12]. Mohammadi Janaki et al. [13] studied the optimized CHP set-up using renewable energies in Rural Health Centers in Iran. Several hybrid procedures are assessed in HOMER software. The energy-technoeconomic-environment efficiency of turbines is evaluated and added to the software database. According to the outcomes, the three scenarios are recognized as solar cell-battery, solar cell-biomass-battery, and solar cell-wind turbine-battery. In the best economic circumstance, 25% of the needed energy is produced by solar cells and the remained 75% is generated by a gas boiler which generates 7,050 kg of CO<sub>2</sub> each year. Smierciew et al. [14] utilized solar energy in the ejector cooling cycle by using isobutene as a working fluid in commercial and industrial buildings. According to the result, the performance coefficient is calculated at about 0.2. Helvacı and Khan [15] performed an energetic assessment on a solar-based organic Rankine cycle considering 24 different refrigerants. According to the outcomes, by employing butane as the refrigerant, the net output power and energy efficiency are calculated 210.45 and 9.54%, respectively. Wang et al. [16] studied hybrid cooling, heating, and power production set-up employing solar resources. The impacts of an hour and aperture angles on the efficiency of the system are demonstrated. They revealed that the efficient aperture angle for June 12 at 10 pm is calculated 60 degrees. Khalid et al. [17] studied the energy and exergy evaluation of a hybrid system equipped with biomass and solar energies. They performed the impact of important factors such as turbine inlet temperature, ambient temperature, and compressor outlet pressure on the whole efficiency of the system. The energy and exergy efficiencies for this set-up are reported 66.5% and 39.7%, respectively. Al-Sulaiman et al. [18] presented a combined cooling, heating, and power (CCHP) system with three managing frameworks. Based on the outcomes, the highest efficiency is reported 15% for the solar-based state, 7% for the

storage-solar-based state, and 6.5% for the storage-based state. Also, the highest CCHP efficiency is reported 94% for the solar-based scenario, 47% for storage-solar-based scenarios, and 42% for the storage-based scenario. Ghorbani et al. [19] suggested a hybrid system for electricity and freshwater generation using liquid natural gas (LNG) recovery driven by solar energy. This system is designed by incorporating the ORC and multi-effect distillation (MED). The energetic efficiency of the ORC is reported 12.47% and the gain ratio of the MED unit is calculated 2.918. Tiwari et al. [20] conducted an energy evaluation on the solar-based ORC by utilizing the zeotropic mixture of Heptane/R245fa. According to the results, the energy and exergy efficiencies are reported 7.8% and 14.38%, respectively. Ebadollahi et al. [21] presented four various dual-loop structures of electricity and cooling cogeneration systems based on the ORC and ERC. They calculated 19.71% and 25.29% for exergy and thermal efficiencies optimal condition by using the n-pentane as a working fluid. From the exergy analysis, the solar collector with 70.04 kW is recognized as the most destructive constituent.

Several recent theoretical and experimental researches have been conducted to investigate the behavior of the solar-driven ejector refrigeration cycle (ERC) [14]. Chen et al. [22] studied the working characteristics of ejectors using R141b, R245fa, and R600a as working fluids. They showed that different working fluids perform distinctively in the ejector refrigeration system in which R141b has the highest COP of the system compared to the others Sag and Ersoy [23] conducted an experimental investigation into the effect of the throat diameter and location of the motive nozzle concerning mixing chamber inlet on the performance of dry-type evaporator ejector system using R134a as a refrigerant. They concluded that the motive nozzle has no optimum position for ejector expander refrigeration systems. The Ejector refrigeration cycle can be also improved by different methods. Such methods are: adding of evaporator sub-cooler on a modified auto-cascade refrigeration cycle, ejector expander refrigeration cycle, etc. [24]. Sag et al. [25] conducted an experimental study on vapor compression refrigerators using R134a as a refrigerant. In their proposed cycle, the ejector was used as an expander instead of an expansion valve. They showed that the COP of the ejector-expander refrigeration cycle was 7.34-12.8% higher than the basic one, while its exergy efficiency was 6.6-11.24% higher than the basic system.

More recently, there have been done many investigations in the domain of combined power and

cooling cycles which produce power and refrigeration, simultaneously [26]. The most interesting one is the combination of the organic Rankine cycle and an ejector refrigeration cycle. This combined cycle has developed based on the first and second laws of thermodynamics definition. Yan et al. [27] presented a solar-driven ejector compression heat pump cycle (SEHPC) for air-source heat pump water heater application. They have investigated the proposed cycle based on the thermodynamic classical laws using R1234yf and R134a as refrigerants. They demonstrated that the largest exergy destruction is produced by the ejector which is about 25.7% of the total system exergy input. Saleh [28] studied the performance of a combined organic Rankine cycle and vapor compression refrigeration (ORC-VCR) system working with low-grade thermal energy. He proposed different working fluids (R1270, R290, RC318, R236fa, R600a, R236ea, R600, R245fa, R1234ze, and R1234yf) which among all of them R600 and R245fa gave the highest COP. He has also examined the effect of key parameters (evaporator, condenser temperature and etc.) on the ORC-VCR system performance. Yang et al. [28] proposed a novel combined power and ejector refrigeration cycle using zeotropic mixture which divided into the power and refrigeration sub-cycles. In their cycle, the turbine exhaust from the organic Rankine cycle entrains the vapor from the ejector refrigeration cycle. They had also demonstrated that the cycle performs better in lower condenser temperatures. Wang et al. [29] presented a new combined cooling and power (CCP) set-up with the geothermal-based ORC and ERC. Thermodynamic and parametric evaluation of the recommended set-up is investigated. According to the outcomes, the energy and exergy efficiencies are calculated 18.16% and 59.16%, respectively. Elakhdar et al. [30] studied the utilization of low-heat solar energy in the CCP structure. The working fluids R245fa, R601a, R123, and R141b are utilized in this set-up. Furthermore, the impacts of the energetic parameters on the system efficiency are performed. According to the results, the acceptable convergence between experimental and theoretical data are observed.

This paper applies three different novel modified combined power and ejector refrigeration cycles (CPERCs- hereafter for more simplification) along with simple CPERC. It is shown that all three modified cycles have better performance compared with the previous ones based upon both thermodynamic classical laws (1st and 2nd laws). The model has been validated by the previous works which showed a great agreement under the same

conditions. R245fa and isobutene are applied to the proposed cycles showing that isobutene is much more appropriate than R245fa for all cycles. Finally, the effect of the different parameters on the proposed cycles has been conducted to scrutinize more tangible rewards from these combinations. Also, in this study, the system is analyzed by implementing solar energy as the main heat source.

## 2. Cycle description

Figures. 1-4 show schematics of simple combined power and ejector refrigeration cycle (CPERC) as well as three modified ones, namely, CPERC with an IHE, regenerative CPERC, and regenerative CPERC with an IHE, with their corresponding P-h diagrams, respectively. These proposed cycles are a combination of organic Rankine cycles (ORCs) and ejector refrigeration cycle (ERC). The motive vapor is generated in the vapor generator which is heated by low-temperature heat sources (here solar energy-Figure 1(a)). Using this thermal energy, the saturated vapor leaves the vapor generator at state 1 and enters the turbine to produce power. This exited vapor enters the ejector as a primary fluid and draws the lower pressure vapor from evaporator (secondary fluid at point 9) into the ejector. It is efficient to create lower pressure in the ejector in the entrance of nozzle in an isentropic process (point 3). Both primary and secondary fluids are then mixed at mixing chamber (point 4) at an isobar process and then enter into the condenser (point 5). This superheated vapor passes through condenser at a constant pressure by rejecting heat to the surrounding. The saturated liquid divided into two streams. One stream goes through throttling valve (point 8) and then enters into the evaporator to produce cooling capacity by absorbing heat from surrounding. The rest of the stream is pumped back to the generator by the means of pump-1 (point 7), completing simple combined power and refrigeration cycle. Figure 1(b) illustrates the simple CPERC thermodynamic P-h diagram corresponding to Figure 1(a). According to this figure, the proposed cycle is divided into two sub-cycles. One follows process 4-5-6-7-1-2-3-4 as a power sub-cycle and the other 4-5-6-8-9-4 as a refrigeration sub-cycle. These two sub-cycles are conjoined together by the ejector. It has been found that the turbine outlet pressure of the proposed cycle is relatively higher than that of the conventional organic Rankine cycle, since the heat input to the vapor generator is not only used to generate power but also used to induce the vapor from the evaporator [31]. Figure 2(a) shows a modified CPERC with an Internal Heat Exchanger (IHE). It

will be demonstrated that efficiency of simple CPERC can be improved by cooling down the outlet vapor of turbine in two stages by the means of an IHE. The corresponding P-h diagram to this cycle contains two sub-cycles of 5-6-7-8-9-1-2-3-4-5 and 5-6-7-10-11-5 as a power and refrigeration sub-cycles, respectively (Figure 2(b)). One can also improve the performance of two previous CPERCs by importing feed fluid heater in an appropriate manner (Figure 3(a)). This cycle is called regenerative CPERC. In this case, thermodynamic P-h diagram corresponds to regenerative CPERC which contains two sub-cycles (Figure 3(b)). One as a power sub-cycle and other as refrigeration sub-cycle which has much more intricate shape. Finally, for a more efficient case, the regenerative CPERC with an IHE is proposed (Figure 4(a)). The schematic of P-h diagram which corresponds to this cycle is also shown in Figure4 (b).

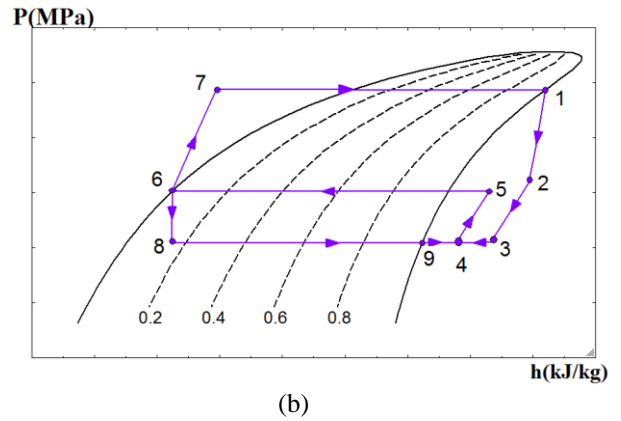
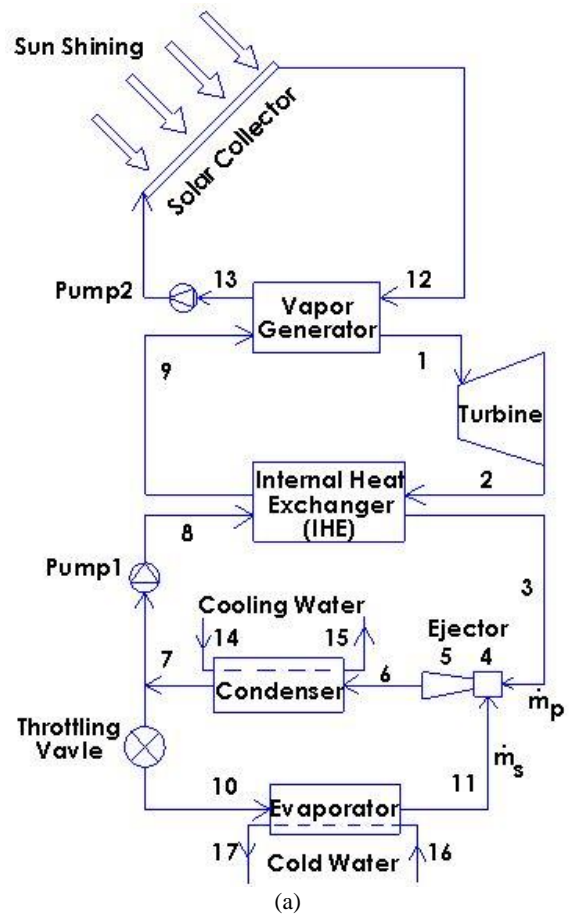
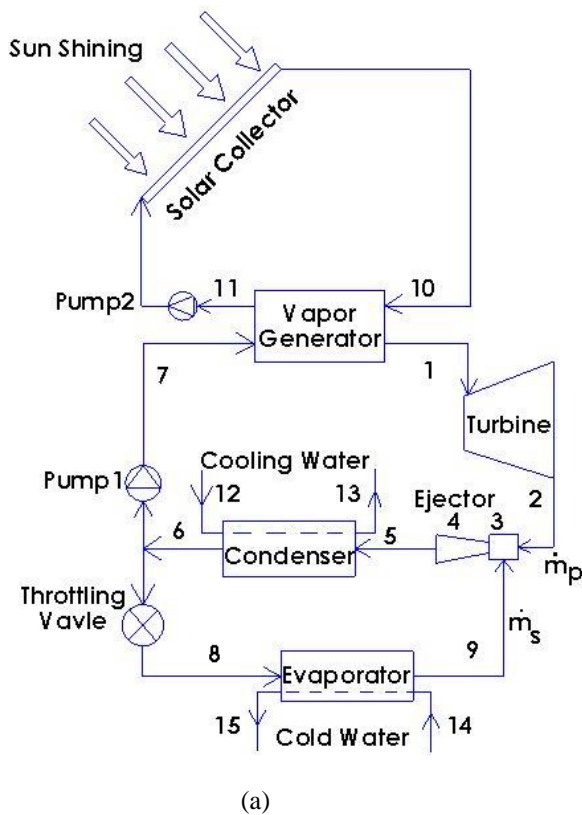


Figure 1 (a). Schematic of simple CPERC and (b). Corresponding thermodynamic P-h diagram.



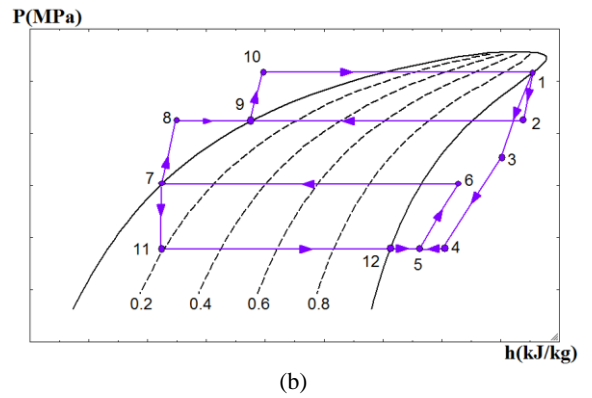
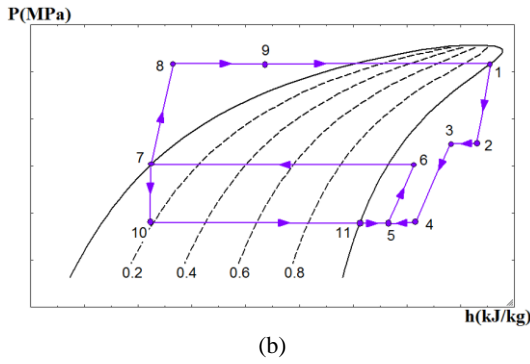
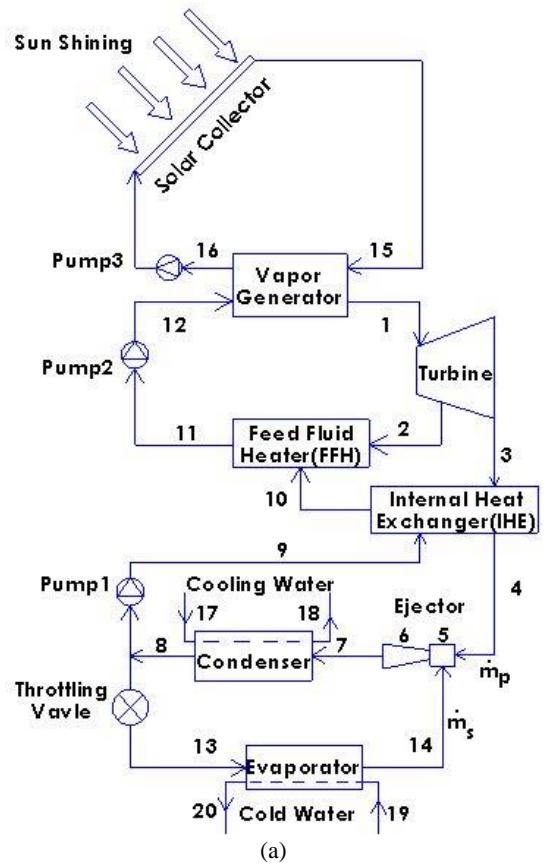
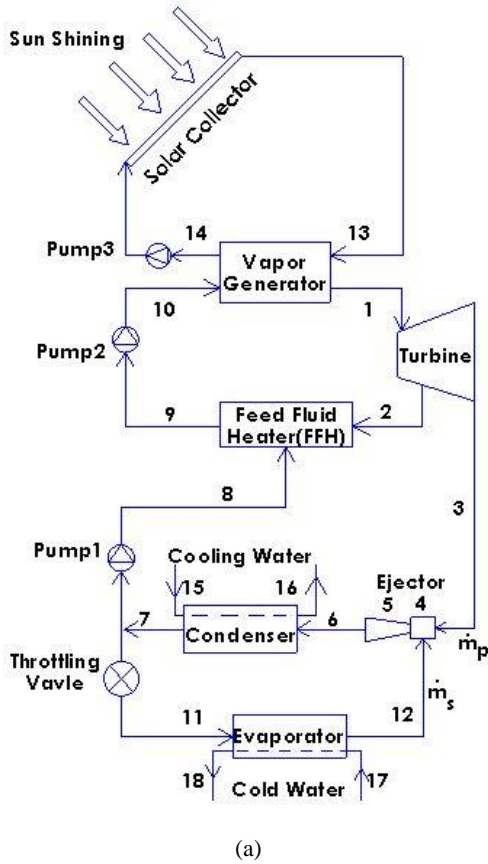


Figure 2 (a). Schematic of CPERC with an IHE and (b). Corresponding thermodynamic P-h diagram.

Figure 3 (a). Schematic of regenerative CPERC and (b). Corresponding thermodynamic P-h diagram.

Table 1. Some thermodynamic properties of selected working fluids [33].

Selected Working fluid	Chemical formula	Critical temperature (°C)	Critical pressure (bar)	Boiling point (°C)	Molecular weight	GWP	ASHARAE safety code
R245fa	C <sub>3</sub> H <sub>3</sub> F <sub>5</sub>	153.86	36.51	15.3	134.05	1030	B1
Isobutene	C <sub>4</sub> H <sub>8</sub>	144.7	40	-6.9	56.1	3	-



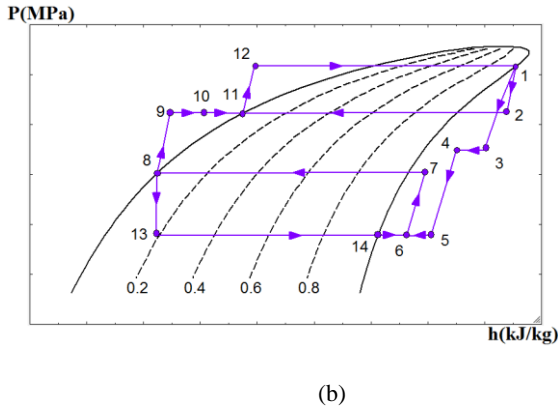


Figure 4 (a). Schematic of regenerative CPERC with an IHE and (b). Corresponding thermodynamic P-h diagram.

### 3. Thermodynamic modelling

The considered working fluids for the proposed combined power and ejector refrigeration cycles are R245fa and isobutene. Among these two refrigerants, R245fa has been proven to be a good candidate for CPERC [31]. The selection of isobutene is more appropriate than R245fa based upon the first and second laws of thermodynamics. Some of the important properties for R245fa and isobutene are given in Table 1. To proceed further, the appropriate input parameters are given in Table 2. These parameters include generator, condenser, and evaporator temperatures and so on. The isentropic efficiencies of pumps and turbine are assumed 95 and 90 %, respectively. The reference temperature and pressure are taken at fixed values of 290 K and 0.101 MPa, respectively. Based upon the refrigeration-dominant production, the power/refrigeration ratio is taken 0.5. For the case of modified regenerative CPERC with and without an IHE, the intermediate pressure is assumed to be 0.65 MPa. Also, the solar energy assumptions are extracted from [21, 32]. In addition to some of the aforesaid parameter values, it is required to consider some general assumptions for the proposed cycles, which are as follows [33, 34]:

- The ejector is modeled as a black-box model. In other words, it is not considered some phenomenon that happens inside this control volume.
- Flow inside the ejector is assumed to be a one-dimensional flow.
- All processes happen at steady state condition.
- There are no pressure drops and heat losses in any equipment and ducts.

- All prescribed flow parameters of the generator, evaporator, condenser, IHE, pumps, FFH, and turbine through whole cycles are assumed to be constant and are in the thermodynamic equilibrium.
- Kinetic energy at the inlet and outlet of all components is negligible.

A program based on the above assumptions has been developed to analyze all proposed cycles' performance. This program has been written in Engineering Equation Solver (EES).

Table 2. Input parameters for energy and exergy analyses of simple CPERC and modified CPERCs [33, 34].

Parameter	value
Generator outlet temperature $T_g$ (K)	395
Condenser outlet temperature $T_c$ (K)	298
Evaporator outlet temperature $T_e$ (K)	270
Turbine isentropic efficiency $\eta_{is,t}$ (%)	90
Pumps isentropic efficiency $\eta_{is,pu}$ (%)	95
Reference state temperature $T_0$ (K)	290
Reference state pressure $P_0$ (MPa)	0.101
Intermediate pressure $P_i$ (MPa)	0.65
Vapor mass flow rate $\dot{m}_v$ (kg.s <sup>-1</sup> )	4.6
Turbine outlet pressure $P$ (MPa)	0.46

### 3.1. Energy analysis

One of the fundamental procedures for the cycle performance evaluation is energy analysis based on the first law of thermodynamics. The Thermodynamics laws in the form of the conservation of mass and energy are applied to each component. The general form of the governing equations for energy analysis of a cycle can be written as follows [35]:

$$\sum \dot{m}_{inlet} - \sum \dot{m}_{outlet} = 0 \tag{1}$$

$$\sum (\dot{m}h)_{inlet} - \sum (\dot{m}h)_{outlet} + \sum \dot{Q}_{inlet} - \sum \dot{Q}_{outlet} + \dot{W} = 0 \tag{2}$$

Some of the resulting thermodynamic relations from the above equations for each cycle have been classified in Tables 3-4.

Table 3. Thermodynamic equations for energetic analysis of simple CPERC and CPERC with an IHE.

Component	Simple CPERC	CPERC with an IHE
	Equation	Equation
Generator duty ( $\dot{Q}_g$ )	$\dot{Q}_g = \dot{m}_1(h_1 - h_7)$	$\dot{Q}_g = \dot{m}_1(h_1 - h_9)$
Turbine power ( $\dot{W}_t$ )	$\dot{W}_t = \dot{m}_1(h_1 - h_2)$	$\dot{W}_t = \dot{m}_1(h_1 - h_2)$
Condenser duty ( $\dot{Q}_c$ )	$\dot{Q}_c = \dot{m}_5(h_5 - h_6)$	$\dot{Q}_c = \dot{m}_6(h_6 - h_7)$
Pump-1 power ( $\dot{W}_{pu1}$ )	$\dot{W}_{pu1} = \dot{m}_7(h_7 - h_6)$	$\dot{W}_{pu1} = \dot{m}_8(h_8 - h_7)$
Cooling capacity of evaporator ( $\dot{Q}_e$ )	$\dot{Q}_e = \dot{m}_9(h_9 - h_8)$	$\dot{Q}_e = \dot{m}_{10}(h_{11} - h_{10})$
Net produced power ( $\dot{W}_{net}$ )	$\dot{W}_{net} = \dot{W}_t - \dot{W}_{pu1}$	$\dot{W}_{net} = \dot{W}_t - \dot{W}_{pu1}$
Thermal efficiency ( $\eta_{th}$ )	$\eta_{th} = (\dot{Q}_e + \dot{W}_{net}) / \dot{Q}_g$	$\eta_{th} = (\dot{Q}_e + \dot{W}_{net}) / \dot{Q}_g$

Table 4 Thermodynamic equations for energetic analysis of regenerative CPERC with and without an IHE.

Component	Regenerative CPERC	Regenerative CPERC with an IHE
	Equation	Equation
Generator duty ( $\dot{Q}_g$ )	$\dot{Q}_g = \dot{m}_1(h_1 - h_{10})$	$\dot{Q}_g = \dot{m}_1(h_1 - h_{12})$
Turbine power ( $\dot{W}_t$ )	$\dot{W}_t = \dot{m}_1 h_1 - \dot{m}_2 h_2 - \dot{m}_3 h_3$	$\dot{W}_t = \dot{m}_1 h_1 - \dot{m}_2 h_2 - \dot{m}_3 h_3$
Condenser duty ( $\dot{Q}_c$ )	$\dot{Q}_c = \dot{m}_6(h_6 - h_7)$	$\dot{Q}_c = \dot{m}_7(h_7 - h_8)$
Pump-1 power ( $\dot{W}_{pu1}$ )	$\dot{W}_{pu1} = \dot{m}_8(h_8 - h_7)$	$\dot{W}_{pu1} = \dot{m}_9(h_9 - h_8)$

Pump-2 power ( $\dot{W}_{pu2}$ )	$\dot{W}_{pu2} = \dot{m}_9(h_{10} - h_9)$	$\dot{W}_{pu2} = \dot{m}_{12}(h_{12} - h_{11})$
Cooling capacity of evaporator ( $\dot{Q}_e$ )	$\dot{Q}_e = \dot{m}_{11}(h_{12} - h_{11})$	$\dot{Q}_e = \dot{m}_{13}(h_{14} - h_{13})$
Net produced power ( $\dot{W}_{net}$ )	$\dot{W}_{net} = \dot{W}_t - \dot{W}_{pu1} - \dot{W}_{pu2}$	$\dot{W}_{net} = \dot{W}_t - \dot{W}_{pu1} - \dot{W}_{pu2}$
Thermal efficiency ( $\eta_{th}$ )	$\eta_{th} = (\dot{Q}_e + \dot{W}_{net}) / \dot{Q}_g$	$\eta_{th} = (\dot{Q}_e + \dot{W}_{net}) / \dot{Q}_g$

In the combined power and refrigeration cycles it is beneficial to introduce the power/refrigeration ratio (R) which defines the combined cycle capability in producing power and refrigeration in compared with each other:

$$R = \dot{W}_t / \dot{Q}_e \tag{3}$$

The expansion ratio of a turbine is another important parameter which is defined as the ratio of turbine inlet pressure to the outlet pressure:

$$\beta = P_{inlet} / P_{outlet} \tag{4}$$

The mass entrainment ratio of the ejector is also another important parameter in the treatment of the ejector as a most interesting device in the recent refrigeration cycles. This parameter is defined as the mass flow rate of the secondary flow ( $\dot{m}_s$ ) to the primary flow ( $\dot{m}_p$ ) [33, 34]:

$$U = \dot{m}_s / \dot{m}_p \tag{5}$$

in which both  $\dot{m}_s$  and  $\dot{m}_p$  are in (kg/s). This ratio is one of the most influential parameter in the ejector refrigeration cycle analysis. Secondary flow circulates through the refrigeration sub-cycle, while primary flow circulates through the power sub-cycle. So, the mass entrainment of the combined power and ejector refrigeration cycle is related to the power/refrigeration ratio (R), as introduced earlier. Also, as a governed energetic relation of the system, the thermal efficiency is calculated by multiplying the net output power and cooling demand per generator capacity (heat generation source) as below:

$$\eta_{th}^{total} = (\dot{Q}_e + \dot{W}_{net}^{tot}) / \dot{Q}_g^s \tag{6}$$

### 3.2. Exergy analysis

The exergy of a steady stream of matter is equal to the maximum amount of obtainable work when the stream is brought from its initial state to the dead state by processes during which the stream may interact only with the environment. Thus, exergy of a stream of matter is a property of two states, the state of the stream and the state of the environment. The exergy of a system of matter can be divided into distinct components. In the absence of magnetic, electrical, nuclear, and surface tension effects, the rate of total exergy of a system ( $\dot{E}_{total}$ ) can be divided into four components: physical exergy rate ( $\dot{E}_{PH}$ ), kinetic exergy rate ( $\dot{E}_{KN}$ ), potential exergy rate ( $\dot{E}_{PT}$ ), and chemical exergy rate ( $\dot{E}_{CH}$ ) [36, 37]:

$$\dot{E}_{total} = \dot{E}_{PH} + \dot{E}_{KN} + \dot{E}_{PT} + \dot{E}_{CH} \quad (7)$$

and the specific exergy can be expressed as:

$$e_{total} = e_{PH} + e_{KN} + e_{PT} + e_{CH} \quad (8)$$

in which

$$e = \frac{\dot{E}}{\dot{m}} \quad (9)$$

The kinetic and potential exergy rates can be set to zero since our system and its components are at rest relative to the environment. Also, because of rare chemical reactions happening and their negligible value compared with the physical exergy in organic materials, one can neglect the rate of chemical exergy. The specific physical exergy of a closed system for different working fluids can be calculated from the following equation [36, 37]:

$$e_{PH} = h - h_0 - T_0(s - s_0) \quad (10)$$

in which  $h$  and  $S$  are specific enthalpy and entropy of the substance, respectively, and  $h_0$  and  $S_0$  are those parameters at the reference state (dead state) of known pressure and temperature of ( $P_0, T_0$ ).

In exergy analysis, according to their definitions, the product represents desired produced results and fuel represents the expended resources to generate the product. Both of these concepts can be expressed in terms of exergy. Considering that, let us express the exergy rate balance for the element  $i$  of a system as [35]:

$$\dot{E}_F^i = \dot{E}_P^i + \dot{E}_D^i + \dot{E}_L^i \quad (11)$$

in which  $\dot{E}_P^i$  and  $\dot{E}_F^i$  are the rate of generated product and supplied fuel of element  $i$ , respectively. On the other hand,  $\dot{E}_L^i$  and  $\dot{E}_D^i$  are the rate of exergy

loss and exergy destruction of element  $i$ , respectively. Assume all outer surface of the system is at constant reference temperature, and then the rate of exergy loss can be neglected. This assumption is so reasonable in many cases. The same equation for the total system can be written as:

$$\dot{E}_F^{total} = \dot{E}_P^{total} + \dot{E}_D^{total} + \dot{E}_L^{total} \quad (12)$$

whereas components are the corresponding ones in a system.

The exergetic efficiency of element  $i$  ( $\eta_{ex}^i$ ) is defined as the ratio of the product exergy of element  $i$  ( $\dot{E}_P^i$ ) to the fuel exergy of the same element ( $\dot{E}_F^i$ ) [35]:

$$\eta_{ex}^i = \dot{E}_P^i / \dot{E}_F^i \quad (13)$$

The total exergetic efficiency of the system can be expressed as the same as equation (14) [36, 37]:

$$\eta_{ex}^{total} = \dot{E}_P^{total} / \dot{E}_F^{total} \quad (14)$$

in which  $\dot{E}_P^{total}$  and  $\dot{E}_F^{total}$  are the total exergy of product and fuel rate, respectively.

In other words, the total product exergy is calculated from the sum of net output power and the evaporator product exergy, as well as the total exergy efficiency, is obtained by dividing this value by the exergy of the generator as a fuel source (equation 15).

$$\eta_{ex}^{total} = (\dot{E}_P^e + \dot{W}_{net}^{tot}) / \dot{E}_F^g \quad (15)$$

Another important parameter in related to the system inefficiencies is the exergy destruction ratio, which is defined as the ratio of exergy destruction of element  $i$  ( $\dot{E}_D^i$ ) to the overall exergy destruction of the system ( $\dot{E}_D^{total}$ ) [35]:

$$y_D^i = \dot{E}_D^i / \dot{E}_D^{total} \quad (16)$$

The influence coefficient of element  $i$  is defined as the ratio of the exergy rate of supplied fuel ( $\dot{E}_F^i$ ) for element  $i$  to the exergy rate of fuel for the total system ( $\dot{E}_F^{total}$ ) [38]:

$$\phi^i = \dot{E}_F^i / \dot{E}_F^{total} \quad (17)$$

This parameter specifies the impact of the element of  $i$  on the efficiency of the system. Table 5 expresses some of the general exergy rates associated to the utilized components in this paper. Tables 6-9 are presented for more detail on the exergy equations for different components of simple CPERC as well as three modified ones.



Table 5. Exergy rates associated with fuel and product for utilized components at the steady state.

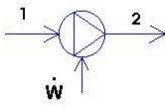
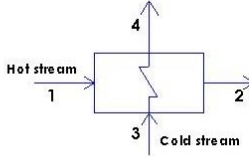
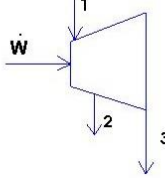
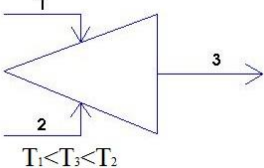
Component	Pump	Heat exchanger	Turbine	Ejector/FFH
Schematic				
Exergy rate of Fuel ( $\dot{E}_F$ )	$\dot{W}$	$\dot{E}_1 - \dot{E}_2$	$\dot{E}_1 - \dot{E}_2 - \dot{E}_3$	$\dot{E}_1 + \dot{E}_2$
Exergy rate of Product ( $\dot{E}_P$ )	$\dot{E}_2 - \dot{E}_1$	$\dot{E}_4 - \dot{E}_3$	$\dot{W}$	$\dot{E}_3$

Table 6. Required equations for exergy analysis of simple CPERC.

Component	Generated product rate ( $\dot{E}_P^i$ )	Fuel supplied rate ( $\dot{E}_F^i$ )	Exergy destruction rate ( $\dot{E}_D^i$ )
Pump-1	$\dot{E}_P^{pu1} = \dot{m}_7(e_7 - e_6)$	$\dot{E}_F^{pu1} = \dot{W}_{pu1}$	$\dot{E}_D^{pu1} = \dot{E}_F^{pu1} - \dot{E}_P^{pu1}$
Generator	$\dot{E}_P^g = \dot{E}_1 - \dot{E}_7$	$\dot{E}_F^g = \dot{E}_{10} - \dot{E}_{11}$	$\dot{E}_D^g = \dot{E}_F^g - \dot{E}_P^g$
Evaporator	$\dot{E}_P^e = \dot{E}_{15} - \dot{E}_{14}$	$\dot{E}_F^e = \dot{E}_8 - \dot{E}_9$	$\dot{E}_D^e = \dot{E}_F^e - \dot{E}_P^e$
Turbine	$\dot{E}_P^t = \dot{W}_t$	$\dot{E}_F^t = \dot{E}_1 - \dot{E}_2$	$\dot{E}_D^t = \dot{E}_F^t - \dot{E}_P^t$
Ejector	$\dot{E}_P^{ej} = \dot{m}_9(e_5 - e_9)$	$\dot{E}_F^{ej} = \dot{m}_2(e_2 - e_5)$	$\dot{E}_D^{ej} = \dot{E}_F^{ej} - \dot{E}_P^{ej}$
Condenser	$\dot{E}_P^c = \dot{E}_{13} - \dot{E}_{12}$	$\dot{E}_F^c = \dot{E}_5 - \dot{E}_6$	$\dot{E}_D^c = \dot{E}_F^c - \dot{E}_P^c$
Total system	$\dot{E}_P^{total} = \dot{E}_P^t - \dot{E}_P^{pu1} + \dot{E}_P^e$	$\dot{E}_F^{total} = \dot{E}_F^g$	$\dot{E}_D^{total} = \sum_{i=1}^n \dot{E}_D^i$

Table 7. Required equations for exergy analysis of CPERC with an IHE.

Component	Generated product rate ( $\dot{E}_P^i$ )	Fuel supplied rate ( $\dot{E}_F^i$ )	Exergy destruction rate ( $\dot{E}_D^i$ )
Pump-1	$\dot{E}_P^{pu1} = \dot{m}_8(e_8 - e_7)$	$\dot{E}_F^{pu1} = \dot{W}_{pu1}$	$\dot{E}_D^{pu1} = \dot{E}_F^{pu1} - \dot{E}_P^{pu1}$
Generator	$\dot{E}_P^g = \dot{E}_1 - \dot{E}_9$	$\dot{E}_F^g = \dot{E}_{12} - \dot{E}_{13}$	$\dot{E}_D^g = \dot{E}_F^g - \dot{E}_P^g$
Evaporator	$\dot{E}_P^e = \dot{E}_{17} - \dot{E}_{16}$	$\dot{E}_F^e = \dot{E}_{10} - \dot{E}_{11}$	$\dot{E}_D^e = \dot{E}_F^e - \dot{E}_P^e$
Turbine	$\dot{E}_P^t = \dot{W}_t$	$\dot{E}_F^t = \dot{E}_1 - \dot{E}_2$	$\dot{E}_D^t = \dot{E}_F^t - \dot{E}_P^t$
Ejector	$\dot{E}_P^{ej} = \dot{m}_{11}(e_6 - e_{11})$	$\dot{E}_F^{ej} = \dot{m}_3(e_3 - e_6)$	$\dot{E}_D^{ej} = \dot{E}_F^{ej} - \dot{E}_P^{ej}$
IHE	$\dot{E}_P^{IHE} = \dot{E}_9 - \dot{E}_8$	$\dot{E}_F^{IHE} = \dot{E}_2 - \dot{E}_3$	$\dot{E}_D^{IHE} = \dot{E}_F^{IHE} - \dot{E}_P^{IHE}$
Condenser	$\dot{E}_P^c = \dot{E}_{15} - \dot{E}_{14}$	$\dot{E}_F^c = \dot{E}_6 - \dot{E}_7$	$\dot{E}_D^c = \dot{E}_F^c - \dot{E}_P^c$
Total system	$\dot{E}_P^{total} = \dot{E}_P^t - \dot{E}_P^{pu1} + \dot{E}_P^e$	$\dot{E}_F^{total} = \dot{E}_F^g$	$\dot{E}_D^{total} = \sum_{i=1}^n \dot{E}_D^i$

Table 8. Required equations for exergy analysis of regenerative CPERC.

Component	Generated product rate ( $\dot{E}_p^i$ )	Fuel supplied rate ( $\dot{E}_F^i$ )	Exergy destruction rate ( $\dot{E}_D^i$ )
Pump-1	$\dot{E}_p^{pu1} = \dot{m}_8(e_8 - e_7)$	$\dot{E}_F^{pu1} = \dot{W}_{pu1}$	$\dot{E}_D^{pu1} = \dot{E}_F^{pu1} - \dot{E}_p^{pu1}$
Pump-2	$\dot{E}_p^{pu2} = \dot{E}_{10} - \dot{E}_9$	$\dot{E}_F^{pu2} = \dot{W}_{pu2}$	$\dot{E}_D^{pu2} = \dot{E}_F^{pu2} - \dot{E}_p^{pu2}$
Generator	$\dot{E}_p^g = \dot{E}_1 - \dot{E}_{10}$	$\dot{E}_F^g = \dot{E}_{13} - \dot{E}_{14}$	$\dot{E}_D^g = \dot{E}_F^g - \dot{E}_p^g$
Evaporator	$\dot{E}_p^e = \dot{E}_{18} - \dot{E}_{17}$	$\dot{E}_F^e = \dot{E}_{11} - \dot{E}_{12}$	$\dot{E}_D^e = \dot{E}_F^e - \dot{E}_p^e$
Turbine	$\dot{E}_p^t = \dot{W}_t$	$\dot{E}_F^t = \dot{E}_1 - \dot{E}_2 - \dot{E}_3$	$\dot{E}_D^t = \dot{E}_F^t - \dot{E}_p^t$
Ejector	$\dot{E}_p^{ej} = \dot{m}_{12}(e_6 - e_{12})$	$\dot{E}_F^{ej} = \dot{m}_3(e_3 - e_6)$	$\dot{E}_D^{ej} = \dot{E}_F^{ej} - \dot{E}_p^{ej}$
FFH	$\dot{E}_p^{FFH} = \dot{m}_8(e_9 - e_8)$	$\dot{E}_F^{FFH} = \dot{m}_2(e_2 - e_9)$	$\dot{E}_D^{FFH} = \dot{E}_F^{FFH} - \dot{E}_p^{FFH}$
Condenser	$\dot{E}_p^c = \dot{E}_{16} - \dot{E}_{15}$	$\dot{E}_F^c = \dot{E}_6 - \dot{E}_7$	$\dot{E}_D^c = \dot{E}_F^c - \dot{E}_p^c$
Total system	$\dot{E}_p^{total} = \dot{E}_p^t - \dot{E}_p^{pu1} - \dot{E}_p^{pu2} + \dot{E}_p^e$	$\dot{E}_F^{total} = \dot{E}_F^g$	$\dot{E}_D^{total} = \sum_{i=1}^n \dot{E}_D^i$

Table 9. Required equations for exergy analysis of regenerative CPERC with an IHE.

Component	Generated product rate ( $\dot{E}_p^i$ )	Fuel supplied rate ( $\dot{E}_F^i$ )	Exergy destruction rate ( $\dot{E}_D^i$ )
Pump-1	$\dot{E}_p^{pu1} = \dot{m}_9(e_9 - e_8)$	$\dot{E}_F^{pu1} = \dot{W}_{pu1}$	$\dot{E}_D^{pu1} = \dot{E}_F^{pu1} - \dot{E}_p^{pu1}$
Pump-2	$\dot{E}_p^{pu2} = \dot{E}_{12} - \dot{E}_{11}$	$\dot{E}_F^{pu2} = \dot{W}_{pu2}$	$\dot{E}_D^{pu2} = \dot{E}_F^{pu2} - \dot{E}_p^{pu2}$
Generator	$\dot{E}_p^g = \dot{E}_1 - \dot{E}_{12}$	$\dot{E}_F^g = \dot{E}_{15} - \dot{E}_{16}$	$\dot{E}_D^g = \dot{E}_F^g - \dot{E}_p^g$
Evaporator	$\dot{E}_p^e = \dot{E}_{20} - \dot{E}_{19}$	$\dot{E}_F^e = \dot{E}_{13} - \dot{E}_{14}$	$\dot{E}_D^e = \dot{E}_F^e - \dot{E}_p^e$
Turbine	$\dot{E}_p^t = \dot{W}_t$	$\dot{E}_F^t = \dot{E}_1 - \dot{E}_2 - \dot{E}_3$	$\dot{E}_D^t = \dot{E}_F^t - \dot{E}_p^t$
Ejector	$\dot{E}_p^{ej} = \dot{m}_{14}(e_7 - e_{14})$	$\dot{E}_F^{ej} = \dot{m}_4(e_4 - e_7)$	$\dot{E}_D^{ej} = \dot{E}_F^{ej} - \dot{E}_p^{ej}$
IHE	$\dot{E}_p^{IHE} = \dot{E}_{10} - \dot{E}_9$	$\dot{E}_F^{IHE} = \dot{E}_3 - \dot{E}_4$	$\dot{E}_D^{IHE} = \dot{E}_F^{IHE} - \dot{E}_p^{IHE}$
FFH	$\dot{E}_p^{FFH} = \dot{m}_{10}(e_{11} - e_{10})$	$\dot{E}_F^{FFH} = \dot{m}_2(e_2 - e_{11})$	$\dot{E}_D^{FFH} = \dot{E}_F^{FFH} - \dot{E}_p^{FFH}$
Condenser	$\dot{E}_p^c = \dot{E}_{18} - \dot{E}_{17}$	$\dot{E}_F^c = \dot{E}_7 - \dot{E}_8$	$\dot{E}_D^c = \dot{E}_F^c - \dot{E}_p^c$
Total system	$\dot{E}_p^{total} = \dot{E}_p^t - \dot{E}_p^{pu1} - \dot{E}_p^{pu2} + \dot{E}_p^e$	$\dot{E}_F^{total} = \dot{E}_F^g$	$\dot{E}_D^{total} = \sum_{i=1}^n \dot{E}_D^i$

#### 4. Model validation

Throughout this investigation, the validation is performed between our theoretical work with [31]. Under same conditions and assumptions and using R245fa as a working fluid of simple combined power and ejector refrigeration cycle, present work shows very good agreement with the results of [31]. This calculated accuracy is believed to be sufficient in most engineering applications. The results of this validation have been summarized in Table 10.

Table 10. Model validation between present work and [31]

Parameter	Present work	[31]	Relative error (%)
Net power/input heat ratio $\dot{W}_{net}/\dot{Q}_g(\%)$	11.0	11.0	0.0
Cooling capacity $\dot{Q}_e(kW)$	58.15	58.7	0.93
Mass entrainment ratio $U$	0.328	0.331	0.9
Net power $\dot{W}_{net}(kW)$	27.69	27.9	0.7
Refrigeration/input heat ratio $\dot{Q}_e/\dot{Q}_g(\%)$	23.121	23.1	0.09
Thermal efficiency $\eta_{th}(\%)$	34.14	34.1	0.11
Exergy efficiency $\eta_{ex}(\%)$	56.92	56.8	0.2

#### 5. Results and discussions

To achieve a comprehensive assessment of the proposed cycles, it is necessary to calculate the thermodynamic characteristics of all cycles at each state. This makes the exergetic and energetic analyses much easier to be conducted. This section presents the calculated results from energetic and exergetic analyses of simple CPERC and three modified ones. Tables 11-14 give thermodynamic flow parameters for simple CPERC as well as three modified ones using R245fa and isobutene as working fluids. These thermodynamic properties include temperature, pressure, enthalpy, entropy, and mass flow rate at each point which is essential for the next steps.

##### 5.1. Energy analysis results

Table 15 gives the results of energetic analysis for simple CPERC as well as three modified CPERCs for

both R245fa and isobutene. It is seen that thermal efficiency has been improved by modification of simple combined power and ejector refrigeration cycle. The maximum obtainable thermal efficiency is 46.95 % using isobutene as a working fluid. Through this modification, thermal efficiency is improved by 7.48 and 5.65 % for R245fa and isobutene, respectively. It is also seen that these successive modifications increase the cooling capacity and net produced power of proposed cycles, successively. As shown in Table 15, the net produced power/input heat ratio ( $\dot{W}_{net}/\dot{Q}_g$ ) and refrigeration/input heat ratio ( $\dot{Q}_e/\dot{Q}_g$ ) for this work are larger than the same values for the combined power and ejector refrigeration cycle proposed by Zheng and Weng [31]. These results show that proposed cycles can produce more power and refrigeration compared with the previous ones. These cycles are more applicable for refrigeration purposes, since the power/refrigeration ratio (R) is smaller than unit. In all proposed cycles, the turbine outlet pressure is higher; so that the vapor can be used to derive a refrigeration cycle. This was true in the previous cycle proposed by [31], too. In addition to increase of the key flow parameters due to cycle modification, introducing isobutene as an appropriate working fluid for CPERCs is another fascinating result which can be deduced from Table 15.

##### 5.2. Exergy analysis results

In addition to energetic analysis, exergetic analysis can be also helpful to determine the system inefficiencies for the conversion processes and subsequently, for reducing the utilized energy values in the whole cycle. In this section, the exergetic evaluation of the proposed cycles is presented for different components and the whole cycles (Tables 16-19). The maximum overall exergetic efficiency has been obtained for regenerative CPERC with an IHE by 55.67 % using isobutene as a working fluid. The overall exergy efficiency of the cycle is improved by 8.97 and 5.58 % for R245fa and isobutene, respectively. On the other hand, the maximum exergy destruction of the system has been corresponded to simple CPERC by the value of 34.73 and 25.93 kW when using R245fa and isobutene, respectively. performance has been enhanced from the second law of thermodynamics point of view, too. Among all components in the proposed cycles, the generator has the highest contribution in exergy losses of the overall cycle which is followed by the ejector.

Table 11. Flow parameters for the simple CPERC and CPERC with an IHE for R245fa.

Point	Simple CPERC					CPERC with an IHE				
	$T (K)$	$P (MPa)$	$h (kJ.kg^{-1})$	$s(kJ.kg^{-1}.K^{-1})$	$\dot{m}(kg.s^{-1})$	$T (K)$	$P (MPa)$	$h (kJ.kg^{-1})$	$s(kJ.kg^{-1}.K^{-1})$	$\dot{m} (kg.s^{-1})$
1	395	2	485.1	1.799	0.7281	395	2	485.1	1.799	0.7532
2	345.3	0.46	461.3	1.807	0.7281	345.3	0.46	461.3	1.807	0.7532
3	288.8	0.04578	418.5	1.807	0.7281	337.5	0.46	452.9	1.783	0.7532
4	284.7	0.04578	414.9	1.795	0.9323	298.8	0.101	425.2	1.783	0.7532
5	311.7	0.147	435.7	1.795	0.9323	293.3	0.101	420.2	1.766	0.9644
6	298	0.147	232.3	1.113	0.9323	302.3	0.147	426.8	1.766	0.9644
7	298.7	2	233.7	1.113	0.7281	298	0.147	232.3	1.113	0.9644
8	270	0.04578	232.3	1.12	0.2042	298.7	2	233.7	1.113	0.7532
9	270	0.04578	402.2	1.749	0.2042	305	2	242.1	1.141	0.7532
10	420	0.101	2770	7.593	4.6	270	0.04578	232.3	1.12	0.2113
11	400	0.101	2730	7.496	4.6	270	0.04578	402.2	1.749	0.2113
12	285	0.101	49.83	0.1782	4.122	420	0.101	2770	7.593	4.6
13	296	0.101	95.85	0.3367	4.122	400	0.101	2730	7.496	4.6
14	278	0.101	20.49	0.07399	1.716	285	0.101	49.83	0.1782	4.076
15	273.2	0.101	0.2724	0.0006234	1.716	296	0.101	95.85	0.3367	4.076
16	-	-	-	-	-	278	0.101	20.49	0.07399	1.775
17	-	-	-	-	-	273.2	0.101	0.2724	0.0006234	1.775

Table 12. Flow parameters for the regenerative CPERC with and without an IHE for R245fa.

Point	Regenerative CPERC					Regenerative CPERC with an IHE				
	$T (K)$	$P (MPa)$	$h (kJ.kg^{-1})$	$s(kJ.kg^{-1}.K^{-1})$	$\dot{m} (kg.s^{-1})$	$T (K)$	$P (MPa)$	$h (kJ.kg^{-1})$	$s(kJ.kg^{-1}.K^{-1})$	$\dot{m} (kg.s^{-1})$
1	395	2	485.1	1.799	0.9849	395	2	485.1	1.799	0.9849
2	354.7	0.65	467.1	1.805	0.2748	354.7	0.65	467.1	1.805	0.2419
3	345.3	0.46	461.3	1.807	0.7101	345.3	0.46	461.3	1.807	0.743
4	288.8	0.04578	418.5	1.807	0.7101	335.7	0.46	450.9	1.777	0.743
5	283.9	0.04578	414.1	1.792	0.9674	278.9	0.04578	409.8	1.777	0.743
6	310.8	0.147	434.9	1.792	0.9674	276.6	0.04578	407.8	1.769	1.003
7	298	0.147	232.3	1.113	0.9674	303.5	0.147	428	1.769	1.003
8	298.2	0.65	232.7	1.113	0.7101	298	0.147	232.3	1.113	1.003
9	345.6	0.65	298.1	1.316	0.9849	298.2	0.65	232.7	1.113	0.743
10	346.4	2	299.3	1.316	0.9849	306	0.65	243	1.147	0.743
11	270	0.04578	232.3	1.12	0.2573	345.6	0.65	298.1	1.316	0.9849
12	270	0.04578	402.2	1.749	0.2573	346.4	2	299.3	1.316	0.9849
13	420	0.101	2770	7.593	4.6	270	0.04578	232.3	1.12	0.2596
14	400	0.101	2730	7.496	4.6	270	0.04578	402.2	1.749	0.2596
15	285	0.101	49.83	0.1782	4.259	420	0.101	2770	7.593	4.6
16	296	0.101	95.85	0.3367	4.259	400	0.101	2730	7.496	4.6
17	278	0.101	20.49	0.07399	2.162	285	0.101	49.83	0.1782	4.264
18	273.2	0.101	0.2724	0.0006234	2.162	296	0.101	95.85	0.3367	4.264
19	-	-	-	-	-	278	0.101	20.49	0.07399	2.181
20	-	-	-	-	-	273.2	0.101	0.2724	0.0006234	2.181

Table 13. Flow parameters for the simple CPERC and CPERC with an IHE for isobutene.

Point	Simple CPERC					CPERC with an IHE				
	$T (K)$	$P (MPa)$	$h (kJ.kg^{-1})$	$s (kJ.kg^{-1}.K^{-1})$	$\dot{m} (kg.s^{-1})$	$T (K)$	$P (MPa)$	$h (kJ.kg^{-1})$	$s (kJ.kg^{-1}.K^{-1})$	$\dot{m} (kg.s^{-1})$
1	395	2.739	532.7	1.502	0.4006	395	2.739	532.7	1.502	0.4148
2	322	0.46	468.4	1.524	0.4006	322	0.46	468.4	1.524	0.4148
3	279.9	0.1186	412.2	1.524	0.4006	313.6	0.46	452.8	1.475	0.4148
4	277.3	0.1186	408	1.509	0.5588	266.7	0.101	392.5	1.475	0.4148
5	305.7	0.302	445.9	1.509	0.5588	267.6	0.101	393.9	1.48	0.5786
6	298	0.302	71.51	0.2528	0.5588	300.7	0.302	437.1	1.48	0.5786
7	298.4	2.739	75.85	0.2535	0.4006	298	0.302	71.51	0.2528	0.5786
8	270	0.1186	71.51	0.2647	0.1582	298.4	2.739	75.85	0.2535	0.4148
9	270	0.1186	397.4	1.471	0.1582	305	2.739	91.47	0.3053	0.4148
10	420	0.101	2770	7.593	4.6	270	0.1186	71.51	0.2647	0.1638
11	400	0.101	2730	7.496	4.6	270	0.1186	397.4	1.471	0.1638
12	285	0.101	49.83	0.1782	4.546	420	0.101	2770	7.593	4.6
13	296	0.101	95.85	0.3367	4.546	400	0.101	2730	7.496	4.6
14	278	0.101	20.49	0.07399	2.55	285	0.101	49.83	0.1782	4.597
15	273.2	0.101	0.2724	0.0006234	2.55	296	0.101	95.85	0.3367	4.597
16	-	-	-	-	-	278	0.101	20.49	0.07399	2.64
17	-	-	-	-	-	273.2	0.101	0.2724	0.0006234	2.64

Table 14. Flow parameters for CPERC regenerative with and without an IHE for isobutene.

Point	Regenerative CPERC					Regenerative CPERC with an IHE				
	$T (K)$	$P (MPa)$	$h (kJ.kg^{-1})$	$s (kJ.kg^{-1}.K^{-1})$	$\dot{m} (kg.s^{-1})$	$T (K)$	$P (MPa)$	$h (kJ.kg^{-1})$	$s (kJ.kg^{-1}.K^{-1})$	$\dot{m} (kg.s^{-1})$
1	395	2.739	532.7	1.502	0.4736	395	2.739	532.7	1.502	0.4736
2	333.1	0.65	481.5	1.519	0.07887	333.1	0.65	481.5	1.519	0.05991
3	322	0.46	468.4	1.524	0.3948	322	0.46	468.4	1.524	0.4137
4	279.9	0.1186	412.2	1.524	0.3948	312.8	0.46	449.7	1.465	0.4137
5	277	0.1186	407.5	1.508	0.5754	270	0.1186	396	1.465	0.4137
6	305.4	0.302	445.4	1.508	0.5754	270	0.1186	396.4	1.467	0.5959
7	298	0.302	71.51	0.2528	0.5754	298.4	0.302	433.2	1.467	0.5959
8	298.1	0.65	74.53	0.2533	0.3948	298	0.302	71.51	0.2528	0.5959
9	326	0.65	142.3	0.478	0.4736	298.1	0.65	74.53	0.2533	0.4137
10	327.3	2.739	146.3	0.4786	0.4736	306	0.65	93.18	0.3176	0.4137
11	270	0.1186	71.51	0.2647	0.1807	326	0.65	142.3	0.478	0.4736
12	270	0.1186	397.4	1.471	0.1807	327.3	2.739	146.3	0.4786	0.4736
13	420	0.101	2770	7.593	4.6	270	0.1186	71.51	0.2647	0.1822
14	400	0.101	2730	7.496	4.6	270	0.1186	397.4	1.471	0.1822
15	285	0.101	49.83	0.1782	4.675	420	0.101	2770	7.593	4.6
16	296	0.101	95.85	0.3367	4.675	400	0.101	2730	7.496	4.6
17	278	0.101	20.49	0.07399	2.912	285	0.101	49.83	0.1782	4.683
18	273.2	0.101	0.2724	0.0006234	2.912	296	0.101	95.85	0.3367	4.683
19	-	-	-	-	-	278	0.101	20.49	0.07399	2.937
20	-	-	-	-	-	273.2	0.101	0.2724	0.0006234	2.937

Table 15 Energy evaluation results obtained from energetic analysis of simple CPERC and modified CPERCs for R245fa and isobutene.

Component	R245fa				Isobutene			
	(a)	(b)	(c)	(d)	(a)	(b)	(c)	(d)
Duty of generator $\dot{Q}_g(kW)$	183	183	183	183	183	183	183	183
Cooling capacity $\dot{Q}_e(kW)$	34.7	35.9	43.72	44.1	51.55	53.38	58.88	59.38
Duty of condenser $\dot{Q}_c(kW)$	189.7	187.6	196	196.2	209.2	211.5	215.2	215.5
Duty of IHE $\dot{Q}_{IHE}(kW)$	-	6.297	-	7.716	-	6.483	-	7.718
Mass entrainment ratio $U$	0.2805	0.2805	0.3623	0.3493	0.3948	0.3948	0.4576	0.4403
Pump-1 power $\dot{W}_{pu1}(kW)$	1.059	1.096	0.2807	0.2937	1.736	1.798	1.191	1.248
Pump-2 power $\dot{W}_{pu2}(kW)$	-	-	1.167	1.167	-	-	1.882	1.882
Turbine power $\dot{W}_t(kW)$	17.35	17.95	21.86	22.05	25.78	26.69	29.44	29.69
Turbine expansion ratio $\beta$	4.349	4.349	4.349	4.349	5.954	5.954	5.954	5.954
Net produced power $\dot{W}_{net}(kW)$	16.29	16.85	20.41	20.59	24.04	24.89	26.37	26.56
Net power/input heat ratio $\dot{W}_{net}/\dot{Q}_g(\%)$	8.901	9.207	11.15	11.25	13.13	13.6	14.41	14.51
Refrigeration/input heat ratio $\dot{Q}_e/\dot{Q}_g(\%)$	18.96	19.61	23.88	24.09	28.16	29.16	32.17	32.44
Thermal efficiency $\eta_{th}(\%)$	27.86	28.82	35.03	35.34	41.3	42.76	46.67	46.95

(a): simple CPERC, (b): CPERC with an IHE (c) CPERC, (d) regenerative CPERC with an IHE.

Table 16. Exergy evaluation of simple CPERC and CPERC with an IHE for R245fa.

Component	Simple CPERC						CPERC with an IHE					
	$E_p^i$ (kW)	$E_f^i$ (kW)	$E_b^i$ (kW)	$y_b^i$ (%)	$\phi^i$ (%)	$\eta_{ex}^i$ (%)	$E_p^i$ (kW)	$E_f^i$ (kW)	$E_b^i$ (kW)	$y_b^i$ (%)	$\phi^i$ (%)	$\eta_{ex}^i$ (%)
Pump-1	1.008	1.059	0.0514	0.148	1.979	95.14	1.043	1.096	0.053	0.156	2.04	95.14
Generator	38.1	53.54	15.44	44.45	100	71.17	39.17	53.54	14.37	42.16	100	73.15
Evaporator	1.814	2.566	0.7518	2.165	4.793	70.7	1.877	2.655	0.777	2.281	4.95	70.7
Condenser	0.3035	5.307	5.003	14.41	9.911	5.719	0.3002	5.013	4.713	13.82	9.36	5.987
Ejector	6.605	18.46	11.86	34.15	34.49	35.77	4.17	15.97	11.8	34.6	29.82	26.12
IHE	-	-	-	-	-	-	0.2469	0.948	0.7012	2.056	1.77	26.04
Turbine	17.35	18.98	1.625	4.679	35.44	91.44	17.95	19.63	1.681	4.93	36.66	91.44
Total system	18.16	53.54	34.73	-	-	33.91	18.78	53.54	34.1	-	-	35.08

### 5.3. Parametric evaluation

A comparative study of energetic and exergetic analyses of simple combined power and ejector refrigeration cycle (CPERC), as well as three modified CPERCs, have been conducted and the results are presented here. These three modified

So, obviously, during this modification, simple combined power and ejector refrigeration cycle. An increase in the generator outlet temperature increases refrigeration more considerably than the power. So, this may result in a rise in the mass entrainment ratio. Figure 7 shows the variation of generator outlet temperature with net power/input heat and

refrigeration/input heat ratios for different cycles using isobutene as a working fluid. Since net power and refrigeration are increased through this modification, and hence net power/input heat and refrigeration/input heat ratios are increased by considering constant input heat for all cycles. In the same way, a rise in the generator outlet temperature also gives rise to the net power and refrigeration.

Figure 8 illustrates the variation of the generator outlet temperature versus the overall exergy destruction rate for proposed cycles and working fluids. Firstly, an increase in the generator outlet temperature has caused a fall in the rate of overall exergy destruction through this successive modification. Secondly, in all proposed cycles it is proved that isobutene has the lowest value of exergy losses compared with R245fa which has been introduced as a suitable working fluid by Zheng and Weng [31]. Thirdly, among all proposed cycles, regenerative CPERC with an IHE reveals the lowest value for exergy destruction. This is the main advantage of the proposed cycles compared with previous ones.

### **5.3.2. Effect of the condenser outlet temperature on the performance**

Figure 9 shows the effect of the condenser outlet temperature on the thermal and exergetic efficiencies of simple CPERC as well as three proposed modified CPERCs using isobutene as working fluid. As shown in this figure, both classical efficiencies have been increased as condenser outlet temperature increases, since rejecting heat is decreased. But this slope of increases is varying from cycle to cycle. The slope of this diagram through the modification has turned out to be gentler than the simple CPERC, and hence the sensitivity of the combined power and ejector refrigeration cycle relative to the condenser outlet temperature is decreased. Figure 10 shows the variation of the condenser outlet temperature versus the ejector mass entrainment ratio for different cycles and working fluids. As it is seen, an increase in the condenser outlet temperature increases the refrigeration sub-cycle mass flow rate, and hence increases the mass entrainment ratio for all cycles and working fluids. It is also shown that isobutene can be

a good candidate for more refrigeration and subsequently, more mass flow rate considerations. Since refrigeration is increased during this state-of-art modification, therefore, the mass flow rate is increased, too.

Figure 11 is plotted to explain the effect of the condenser outlet temperature on the net power/input heat and refrigeration/input heat ratios. Since all external conditions are the same for all cycles, then the input heat received from the generator is constant, too. So, it is sufficient to take net power and refrigeration into our consideration. The rate of variation for this parameter with net power and refrigeration varies from cycle to cycle. But as mentioned earlier, on account for a rise in the power and refrigeration in the proposed cycles by decreasing rejecting heat to the environment, condenser outlet temperature increases the net power and refrigeration/input heat ratios.

For achieving a more tangible sense of this modification, the effect of the condenser outlet temperature on the exergy destruction of the overall systems has been investigated (Figure 12). Needless to say, this is one of the main reasons for exergetic analysis which has been conducted through this study. As it is shown, an increase in the condenser outlet temperature decreases the inefficiencies of all proposed cycles, gently. It is also demonstrated that all cycles with isobutene have distinctive lower losses during operation than R245fa.

### **5.3.3. Effect of the evaporator outlet temperature on the performance**

The thermal and exergetic efficiencies of the proposed cycles do not vary with the evaporator outlet temperature. An increase in the evaporator outlet temperature decreases the mass flow rate of the secondary flow under the fixed external conditions consideration. This decreases the mass entrainment ratio by an increase of the evaporator temperature (Figure 13). Another way to reduce the inefficiency of the CPERC is to decrease the evaporator outlet temperature (Figure 14). Of course, this variation is so subtle, since parameters of evaporator have the lowest effect on the cycles among all components.

Table 17. Exergy evaluation of regenerative CPERC with and without an IHE for R245fa.

Component	Regenerative CPERC						Regenerative CPERC with IHE					
	$E_p^i$ (kW)	$E_F^i$ (kW)	$E_D^i$ (kW)	$y_D^i$ (%)	$\phi^i$ (%)	$\eta_{ex}^i$ (%)	$E_p^i$ (kW)	$E_F^i$ (kW)	$E_D^i$ (kW)	$y_D^i$ (%)	$\phi^i$ (%)	$\eta_{ex}^i$ (%)
Pump-1	0.267	0.2807	0.0136	0.045	0.524	95.13	0.279	0.293	0.0142	0.047	0.5486	95.13
Pump-2	1.119	1.167	0.0488	0.162	2.18	95.81	1.119	1.167	0.0488	0.163	2.18	95.81
Generator	45.07	53.54	8.468	28.2	100	84.19	45.07	53.54	8.468	28.4	100	84.19
Evaporator	2.286	3.233	0.9471	3.155	6.038	70.7	2.306	3.261	0.955	3.204	6.091	70.7
Condenser	0.3136	5.451	5.137	17.11	10.18	5.754	0.314	5.263	4.949	16.6	9.829	5.96
Ejector	5.19	15.64	10.45	34.79	29.21	33.19	5.136	15.5	10.37	34.77	28.96	33.13
IHE	-	-	-	-	-	-	0.3087	1.144	0.834	2.8	2.136	26.99
FFH	4.573	7.502	2.929	9.755	14.01	60.96	4.477	6.604	2.127	7.134	12.33	67.79
Turbine	21.86	23.89	2.034	6.775	44.62	91.49	22.05	24.1	2.054	6.888	45.02	91.48
Total system	22.76	53.54	30.02	-	-	42.51	22.96	53.54	29.82	-	-	42.88

Table 18. Exergy evaluation of simple CPERC and CPERC with an IHE for isobutene.

Component	Simple CPERC						CPERC with an IHE					
	$E_p^i$ (kW)	$E_F^i$ (kW)	$E_D^i$ (kW)	$y_D^i$ (%)	$\phi^i$ (%)	$\eta_{ex}^i$ (%)	$E_p^i$ (kW)	$E_F^i$ (kW)	$E_D^i$ (kW)	$y_D^i$ (%)	$\phi^i$ (%)	$\eta_{ex}^i$ (%)
Pump-1	1.652	1.736	0.0843	0.325	3.243	95.14	1.71	1.798	0.087	0.35	3.358	95.14
Generator	37.99	53.54	15.55	59.98	100	70.96	39.09	53.54	14.46	57.93	100	73
Evaporator	2.695	3.77	1.074	4.144	7.041	71.5	2.791	3.903	1.112	4.458	7.29	71.5
Condenser	0.3348	5.596	5.262	20.3	10.45	5.98	0.338	5.574	5.235	20.98	10.41	6.073
Ejector	25.19	26.55	1.36	5.246	49.58	94.88	6.047	7.11	1.062	4.257	13.28	85.06
IHE	-	-	-	-	-	-	0.2515	0.567	0.315	1.264	1.05	44.36
Turbine	25.78	28.37	2.595	10.01	52.99	90.85	26.69	29.37	2.687	10.77	54.86	90.85
Total system	26.82	53.54	25.93	-	-	50.09	27.77	53.54	24.96	-	-	51.86



Table 19. Exergy evaluation of regenerative CPERC with and without an IHE for isobutene.

Component	Regenerative CPERC						Regenerative CPERC with IHE					
	$E_p^i$ (kW)	$E_F^i$ (kW)	$E_D^i$ (kW)	$y_D^i$ (%)	$\phi^i$ (%)	$\eta_{ex}^i$ (%)	$E_p^i$ (kW)	$E_F^i$ (kW)	$E_D^i$ (kW)	$y_D^i$ (%)	$\phi^i$ (%)	$\eta_{ex}^i$ (%)
Pump-1	1.131	1.191	0.06	0.261	2.225	94.93	1.185	1.248	0.0633	0.276	2.332	94.93
Pump-2	1.799	1.882	0.083	0.36	3.515	95.57	1.799	1.882	0.0833	0.364	3.515	95.57
Generator	42.48	53.54	11.06	47.82	100	79.35	42.48	53.54	11.06	48.28	100	79.35
Evaporator	3.079	4.306	1.227	5.306	8.042	71.5	3.105	4.342	1.238	5.403	8.11	71.5
Condenser	0.344	5.748	5.404	23.37	10.74	5.98	0.344	5.665	5.32	23.23	10.58	6.087
Ejector	6.735	7.165	0.429	1.857	13.38	94.01	6.704	7.056	0.3524	1.539	13.18	95.01
IHE	-	-	-	-	-	-	0.003	0.6528	0.6491	2.834	1.219	0.57
FFH	1.025	2.939	1.915	8.279	5.49	34.86	1.07	2.233	1.162	5.075	4.17	47.93
Turbine	29.44	32.39	2.949	12.75	60.49	90.89	29.69	32.67	2.978	13	61.01	90.88
Total system	30.78	53.54	23.13	-	-	55.26	29.81	53.54	22.9	-	-	55.67

Figure 15 shows the effect of the power/refrigeration ratio on the thermal and exergetic efficiencies of simple CPERC as well as three modified CPERCs. As shown in Fig. 15, for refrigeration-dominant combined power and ejector refrigeration cycles, both thermal and exergetic efficiencies are higher than the same corresponding obtained parameters for power-dominant CPERCs. Since in this paper we have chosen  $R=0.5$  (refrigeration-dominant CPERC), both thermal and exergetic efficiencies have been increased compared with the results of [31]. This figure also restates that regenerative CPERC is the most efficient cycle among all proposed CPERCs based upon the first and second laws of thermodynamics. It was mentioned earlier that the power/refrigeration ratio is in inverse relation to the mass entrainment ratio in CPERCs.

The mass flow rate of the secondary flow circulates in the refrigeration sub-cycle and is related to this parameter, directly. In the same manner, the mass flow rate of the primary flow has a direct relation to the power produced in the power sub-cycle. This is why the mass entrainment ratio has decreased with an increase in the power/refrigeration ratio as shown in Figure 16.

Through investigation of the power/refrigeration ratio, it is shown that net produced power remained constant which is different from the power produced by a turbine (Figure 17). Obviously, from a refrigeration-dominant production point of view, regenerative CPERC with and without an IHE is demonstrated to be appropriate cycles among all proposed cycles. More investigation on the power/refrigeration ratio also reveals that this parameter affects exergy destruction, so slightly (Figure 18). For power-dominant cycles ( $R>1$ ) exergy losses are bigger than the refrigeration-dominant cycles ( $R<1$ ).

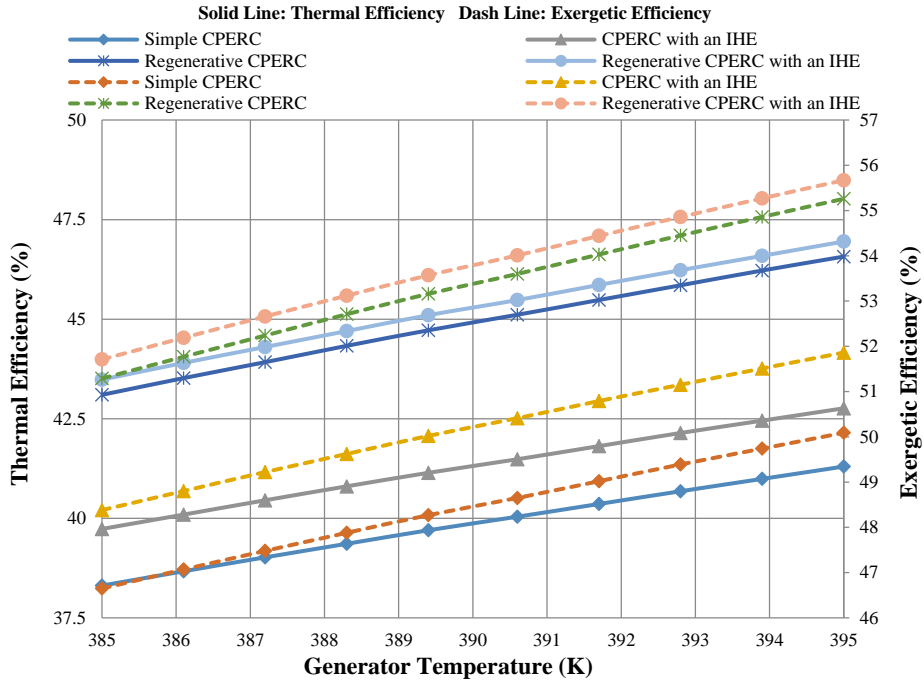


Figure 5. Effect of the generator outlet temperature on the thermal and exergetic efficiencies of simple CPERC and three modified ones for isobutene.

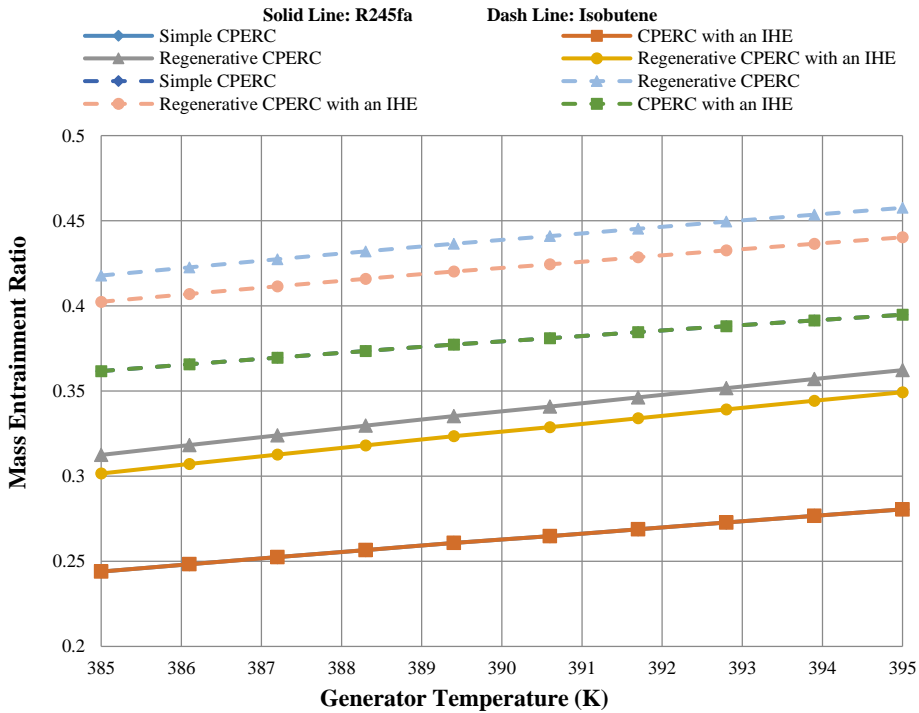


Figure 6. Effect of the generator outlet temperature on mass entrainment ratio of different cycles for R245fa and isobutene.

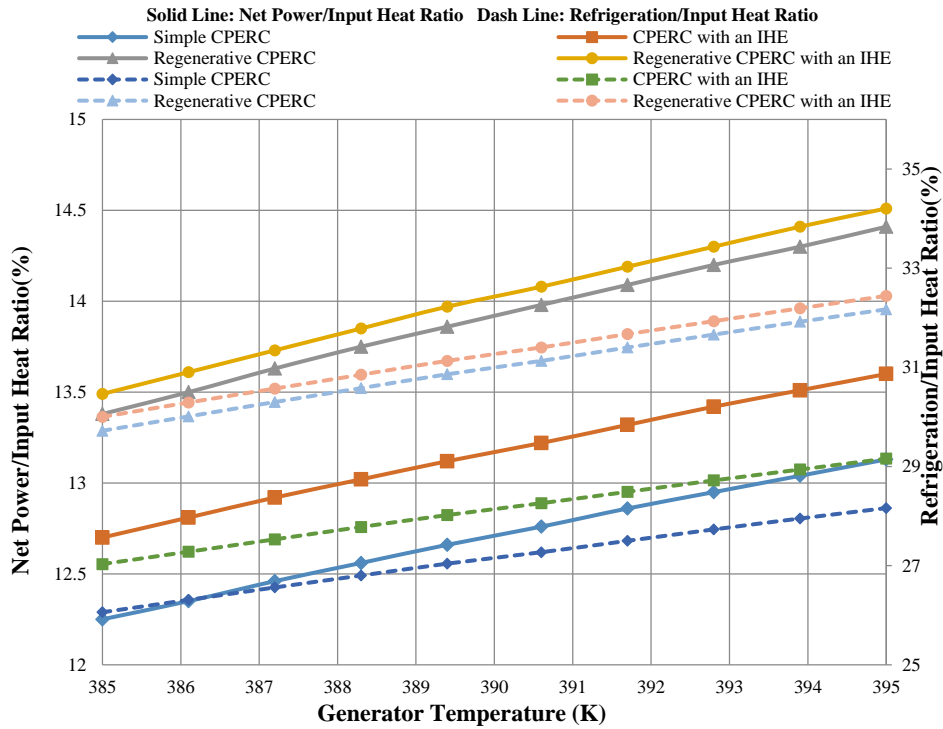


Figure 7. Effect of the generator outlet temperature on the net power/input heat and refrigeration/input heat ratios for different cycles using isobutene.

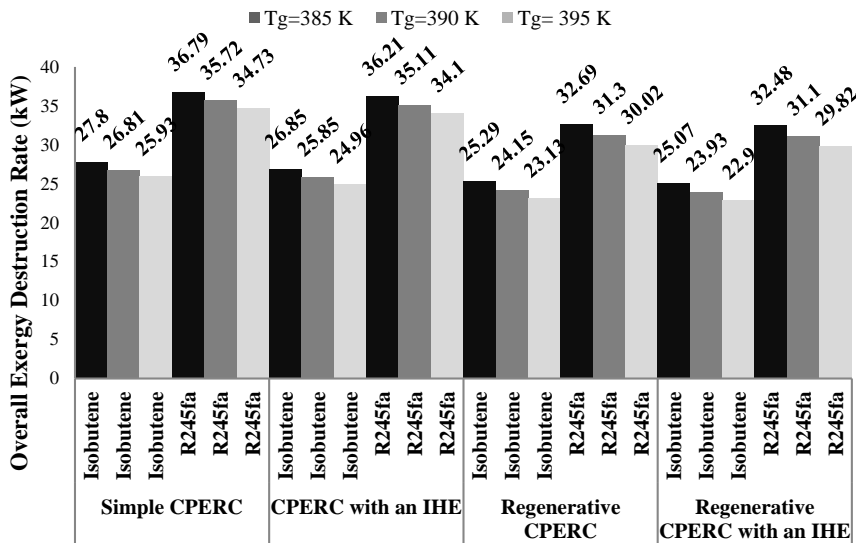


Figure 8. Variation of overall exergy destruction rate versus of the generator outlet temperature for different cycles and working fluids.

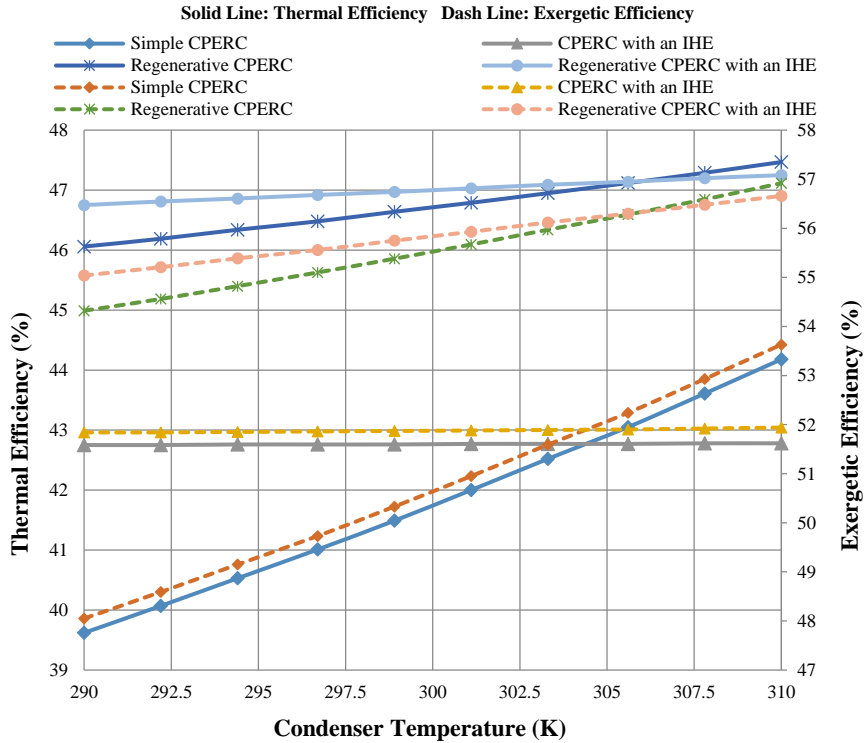


Figure 9. Effect of the condenser outlet temperature on the thermal and exergetic efficiencies

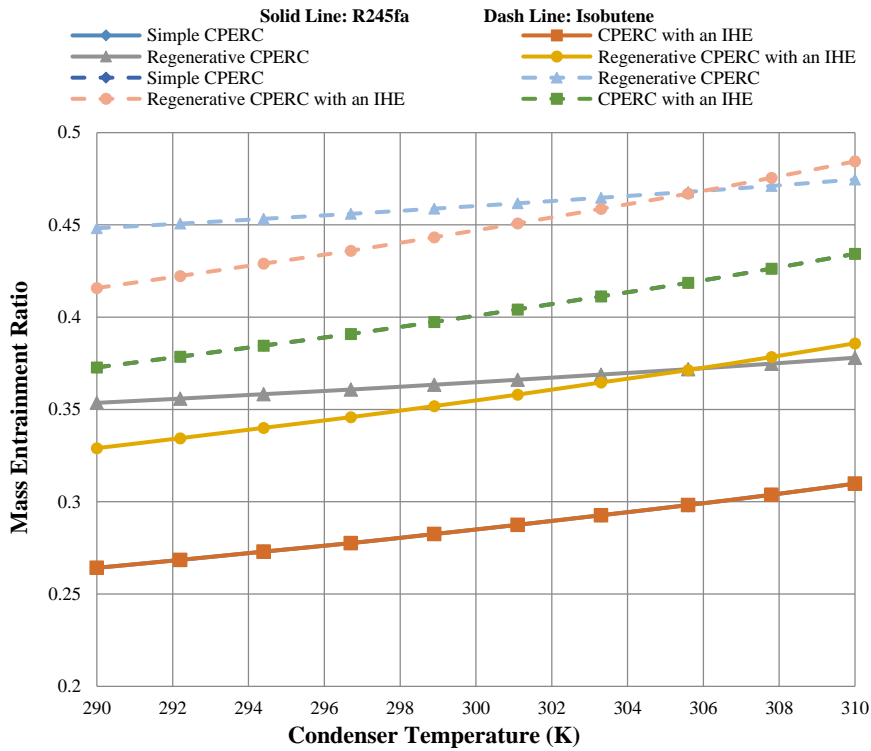


Figure 10. Effect of the condenser outlet temperature on mass entrainment ratio for different cycles.

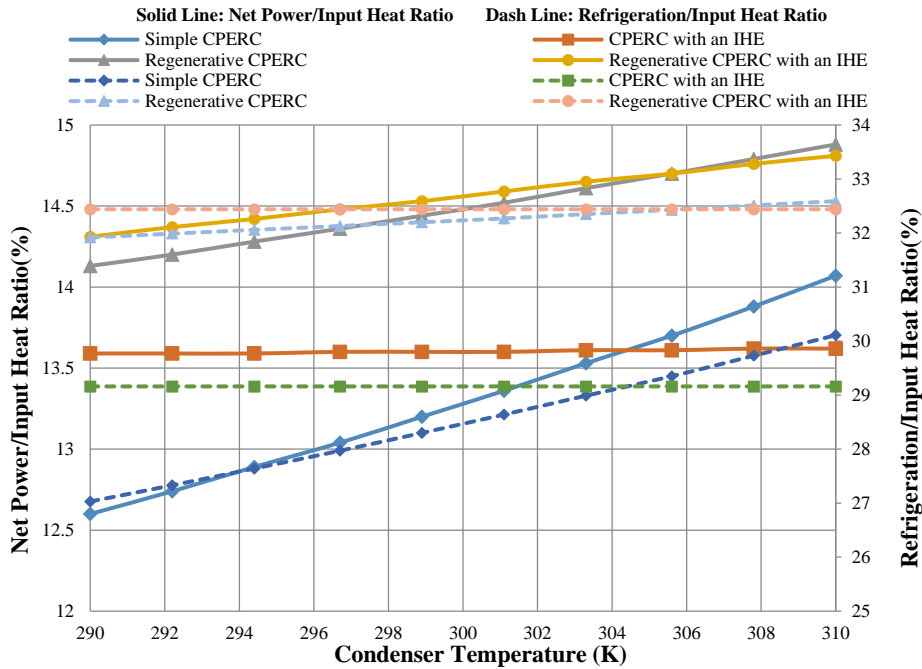


Figure 11. Effect of the condenser outlet temperature on the net power/input heat and refrigeration/input heat ratios for different cycles using isobutene.

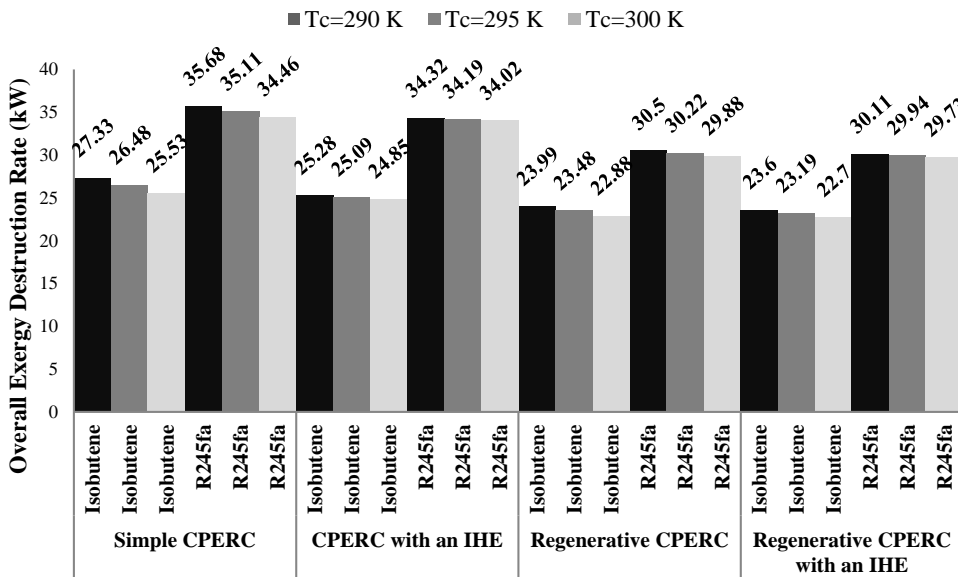


Figure 12. Variation of overall exergy destruction rate versus the condenser outlet temperature for different cycles and working fluids.

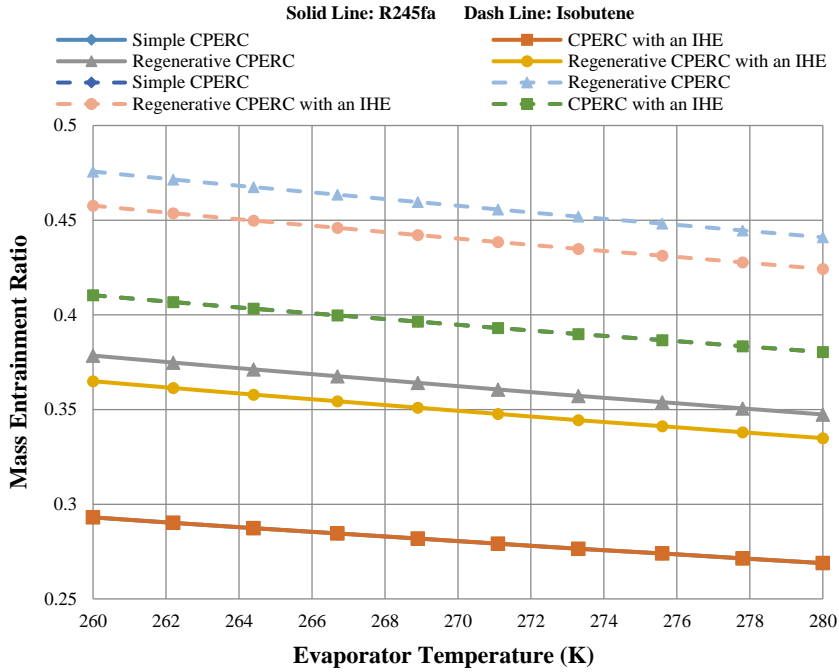


Figure 13. Effect of the evaporator outlet temperature on mass entrainment ratio for different cycles and working fluids.

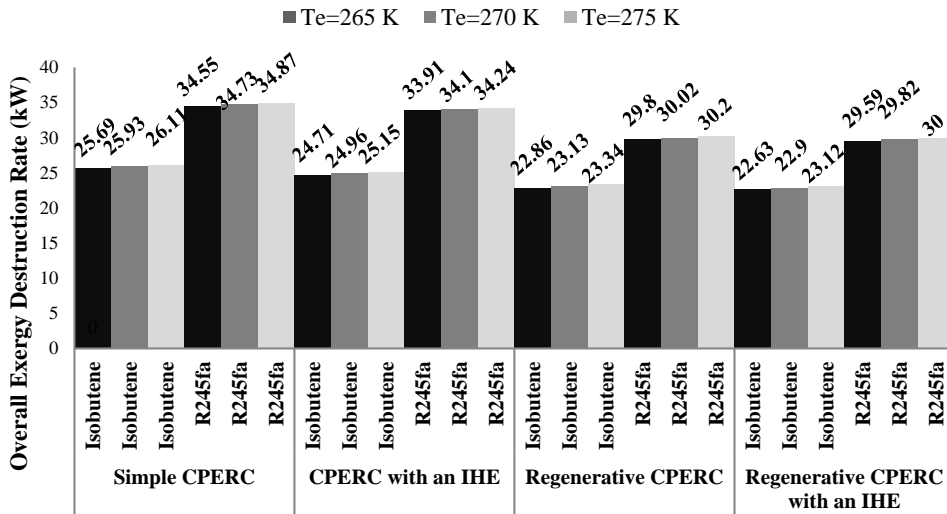


Figure 14. Variation of the overall exergy destruction rate versus the evaporator outlet temperature for different cycles and working fluids.

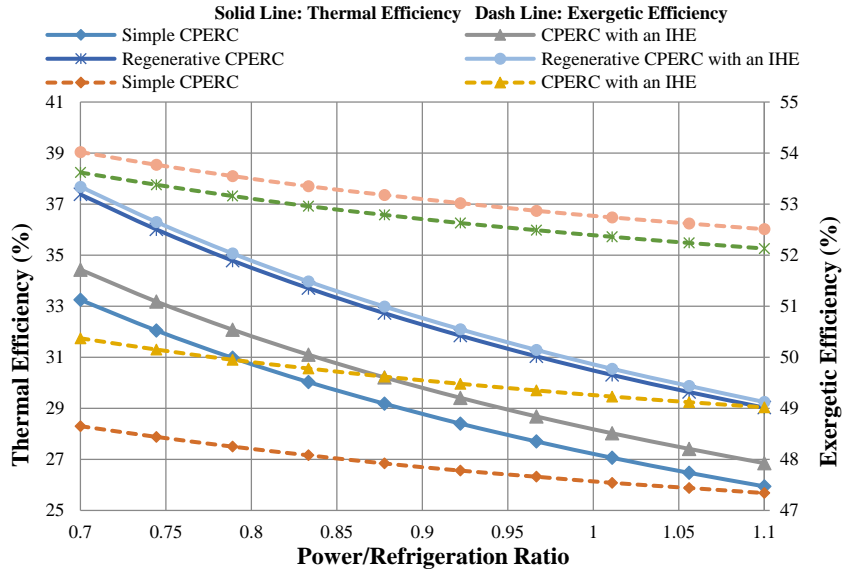


Figure. 15 Effect of the power/refrigeration ratio on the thermal and exergetic efficiencies for different cycles with isobutene.

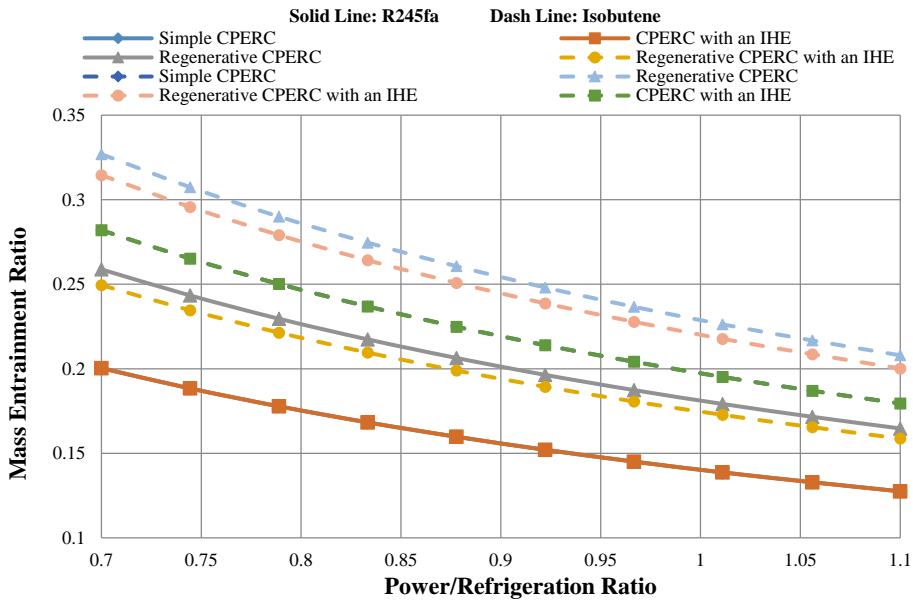


Figure 16. Effect of the power/refrigeration ratio on mass entrainment ratio for different cycles and working fluids.

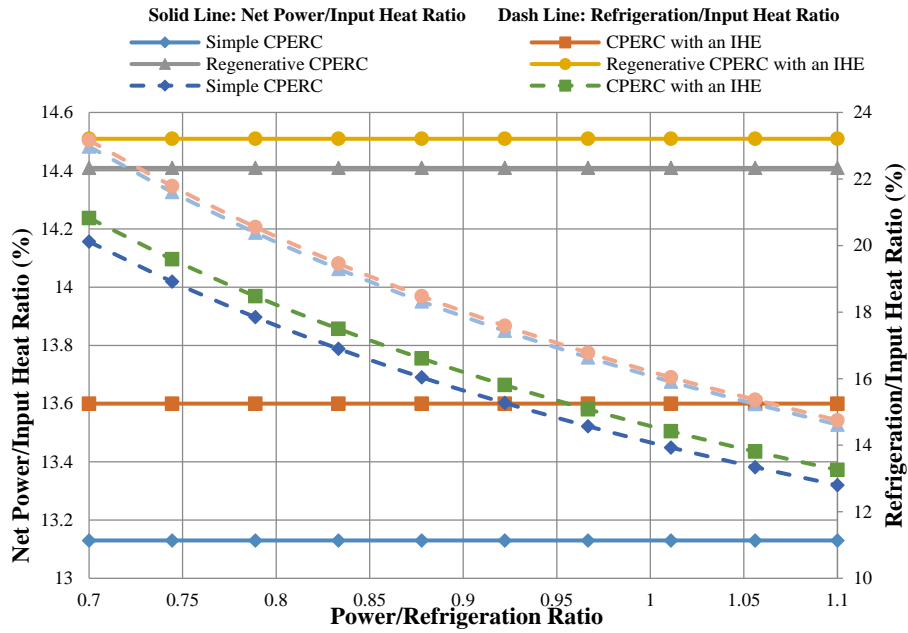


Figure 17. Effect of the power/refrigeration ratio on the net power/input heat and refrigeration/input heat ratios for different cycles using isobutene.

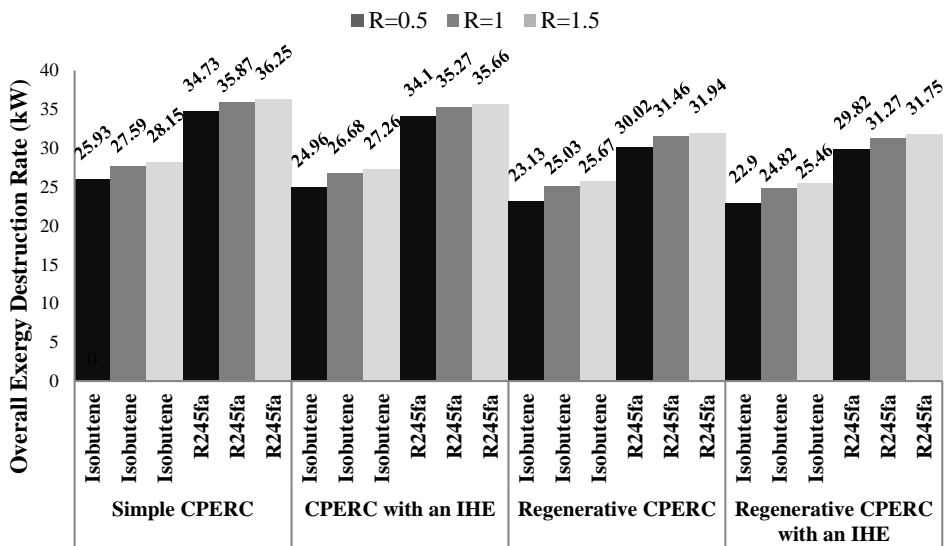


Figure 18. Variation of the overall exergy destruction rate versus the power/refrigeration ratio for different cycles and working fluids.



## 6. Conclusions

Three novel solar-driven modified combined power and ejector refrigeration cycles (MCPERCs) have been proposed to enhance the conventional combined power and ejector refrigeration cycles (CCPERCs) performance. In all of these proposed cycles, the ejector is driven by exited exhaust from the turbine to produce more power and refrigeration, simultaneously. These cycles specifically apply to low-temperature heat sources. Energetic and exergetic analyses are performed for the calculation of the thermodynamic performances using R245fa and isobutene as suitable working fluids. The effect of some key parameters on the cycle's performances has been investigated based on the 1st and 2nd laws of thermodynamics. It is shown that these appropriate proposed cycles can be the best compared to the previous ones for power and refrigeration applications using low-temperature heat sources. From the acquired results the following conclusions can be made.

- The maximum thermal and exergetic efficiencies were obtained for modified regenerative CPERC with an IHE by 46.95 and 55.67 %, respectively, using isobutene as a working fluid.
- The thermal efficiency, a net produced power, cooling capacity, and generator duty are constant concerning the condenser and evaporator outlet temperature variation.
- The increase in the condenser and evaporator outlet temperatures increased and decreased the mass entrainment ratio of the ejector, respectively.
- For power-dominant and refrigeration-dominant production CPERCs, it is sufficient to decrease and increase the mass entrainment ratio, respectively.
- Modified combined power and ejector refrigeration cycles revealed a little more power/refrigeration ratio compared with a simple one. So, modified CPERCs are more suitable for power production than refrigeration ones.
- Regenerative CPERC with an IHE was introduced as the most efficient CPERC among all proposed CPERCs based on the first and second laws of thermodynamics.
- An increase in the generator outlet temperature can be a good choice for an increase of the thermal and exergetic efficiencies in all proposed cycles.

- In all proposed cycles, the generator has the highest exergy destruction ratio, falling into the range of (29.82-34.73) and (22.9-25.93) kW for R245fa and isobutene, respectively.
- An increase in the condenser and generator outlet temperature in all cycles reduced the exergy destruction rate, substantially. However, the decrease in the evaporator temperature decreased the exergy destruction rate for all proposed cycles.

## Nomenclature

### Symbols

<i>APS</i>	Absorption Power System
<i>CCP</i>	Combined Cooling and Power
<i>EES</i>	Engineering Equation Solver
<i>ERC</i>	Ejector Refrigeration Cycle
$\dot{E}$	exergy rate (kW)
<i>e</i>	specific exergy (kJ. kg <sup>-1</sup> )
<i>h</i>	specific enthalpy(kJ. kg <sup>-1</sup> )
$\dot{m}$	mass flow rate (kg. s <sup>-1</sup> )
<i>KC</i>	Kalina Cycle
<i>LNG</i>	Liquid Natural Gas
<i>MED</i>	Multi Effect Distillation
<i>ORC</i>	Organic Rankine Cycle
<i>P</i>	pressure (MPa)
$\dot{Q}$	heat transfer rate (kW)
<i>R</i>	power/refrigeration ratio
<i>s</i>	specific entropy (kJ. kg <sup>-1</sup> . K <sup>-1</sup> )
<i>T</i>	temperature (K)
<i>U</i>	mass entrainment ratio
<i>VCR</i>	Vapor Compression Refrigeration
<i>w</i>	Power (kW)
<i>y</i>	exergy destruction ratio (%)

### Greek letters

$\eta$	efficiency (%)
$\beta$	turbine expansion ratio
$\phi$	influence coefficient (%)

### Subscripts and superscripts

<i>CH</i>	chemical
<i>c</i>	condenser
<i>D</i>	destruction
<i>e</i>	evaporator

<i>ej</i>	ejector
<i>F</i>	fuel
<i>FFH</i>	feed fluid heater
<i>ex</i>	exergetic
<i>g</i>	generator
<i>pu</i>	pump
<i>I</i>	intermediate
<i>IHE</i>	internal heat exchanger
<i>inlet</i>	inlet
<i>KN</i>	kinetical
<i>L</i>	loss
<i>net</i>	net value
<i>P</i>	product
<i>outlet</i>	outlet
<i>p</i>	primary flow
<i>PH</i>	physical
<i>PT</i>	potential
<i>s</i>	secondary flow
<i>t</i>	turbine
<i>total</i>	total of system
<i>v</i>	vapor
<i>1, 2, ...</i>	cycle states
<i>0</i>	dead state

## References

- Mohammadi, F.J.J.o.S.E.R., Design, analysis, and electrification of a solar-powered electric vehicle. 2018. **3**(4): p. 293-299.
- Dincer, I.J.R. and s.e. reviews, Renewable energy and sustainable development: a crucial review. 2000. **4**(2): p. 157-175.
- Xu, X., et al., Policy analysis for grid parity of wind power generation in China. 2020. **138**: p. 111225.
- Bezaatpour, M. and H.J.R.E. Rostamzadeh, Design and evaluation of flat plate solar collector equipped with nanofluid, rotary tube, and magnetic field inducer in a cold region. 2021. **170**: p. 574-586.
- Bezaatpour, M., H. Rostamzadeh, and J.J.J.o.C.P. Bezaatpour, Hybridization of rotary absorber tube and magnetic field inducer with nanofluid for performance enhancement of parabolic trough solar collector. 2021. **283**: p. 124565.
- Chen, C., M. Pinar, and T. Stengos, Determinants of renewable energy consumption: Importance of democratic institutions. *Renewable Energy*, 2021. **179**: p. 75-83.
- Ezzedine, A., G.R. Mohtashami Borzadaran, and A.J.J.o.S.E.R. Rezaei Roknabadi, The Influence of the Geographical Location on the Preventive Replacement of Renewable Energy Devices. 2021. **6**(4): p. 887-897.
- Mohsenipour, M., et al., Design and evaluation of a solar-based trigeneration system for a nearly zero energy greenhouse in arid region. *Journal of Cleaner Production*, 2020. **254**: p. 119990.
- Borzabadi Farahani, M., A. Davodabadi Farahani, and A.J.J.o.S.E.R. Hajizadeh Aghdam, Thermoeconomic Analysis of an Ammonia-water mixture CCHP Cycle with Solar Collectors. 2020. **5**(4): p. 548-559.
- Mohsenipour, M., et al., Design and evaluation of a solar-based trigeneration system for a nearly zero energy greenhouse in arid region. 2020. **254**: p. 119990.
- Farahani, S.D., M. Borzabadi Farahani, and A.J.J.o.S.E.R. Sajedi, Thermodynamic Analysis of ORC-GT Hybrid Cycle and Thermal Recovery from Photovoltaic Panels. 2022. **7**(4): p. 1198-1210.
- Moltames, R., et al., Simulation and Optimization of a Solar Based Trigeneration System Incorporating PEM Electrolyzer and Fuel Cell. 2021. **6**(1): p. 664-677.
- Mohamadi Janaki, D., et al., Optimal Selection and Economical Ranking of Isolated Renewable-based CHP Microgrid in Cold Climate, a Case Study for a Rural Healthcare Center. 2022. **7**(4): p. 1143-1158.
- Śmierciew, K., et al., Experimental investigations of solar driven ejector air-conditioning system. *Energy and buildings*, 2014. **80**: p. 260-267.
- Helvaci, H. and Z. Khan, Thermodynamic modelling and analysis of a solar organic Rankine cycle employing thermofluids. *Energy Conversion and Management*, 2017. **138**: p. 493-510.
- Wang, J., et al., A new combined cooling, heating and power system driven by solar energy. *Renewable Energy*, 2009. **34**(12): p. 2780-2788.
- Khalid, F., I. Dincer, and M.A. Rosen, Energy and exergy analyses of a solar-

- biomass integrated cycle for multigeneration. *Solar Energy*, 2015. **112**: p. 290-299.
18. Al-Sulaiman, F.A., F. Hamdullahpur, and I. Dincer, Performance assessment of a novel system using parabolic trough solar collectors for combined cooling, heating, and power production. *Renewable Energy*, 2012. **48**: p. 161-172.
  19. Ghorbani, B., et al., Introducing a hybrid renewable energy system for production of power and fresh water using parabolic trough solar collectors and LNG cold energy recovery. *Renewable energy*, 2020. **148**: p. 1227-1243.
  20. Tiwari, D., et al., Thermodynamic analysis of Organic Rankine cycle driven by reversed absorber hybrid photovoltaic thermal compound parabolic concentrator system. *Renewable Energy*, 2020. **147**: p. 2118-2127.
  21. Ebadollahi, M., et al., Thermal and exergetic performance enhancement of basic dual-loop combined cooling and power cycle driven by solar energy. *Thermal Science and Engineering Progress*, 2020. **18**: p. 100556.
  22. Chen, J., H. Havtun, and B.J.A.T.E. Palm, Parametric analysis of ejector working characteristics in the refrigeration system. 2014. **69**(1-2): p. 130-142.
  23. Sag, N.B., H.K.J.E.C. Ersoy, and Management, Experimental investigation on motive nozzle throat diameter for an ejector expansion refrigeration system. 2016. **124**: p. 1-12.
  24. Chen, J., J. Yu, and G.J.A.T.E. Yan, Performance analysis of a modified autocascade refrigeration cycle with an additional evaporating subcooler. 2016. **103**: p. 1205-1212.
  25. Sag, N.B., et al., Energetic and exergetic comparison of basic and ejector expander refrigeration systems operating under the same external conditions and cooling capacities. 2015. **90**: p. 184-194.
  26. Kasaeian, A., A. Shamaeizadeh, and B. Jamjoo, Combinations of Rankine with ejector refrigeration cycles: Recent progresses and outlook. *Applied Thermal Engineering*, 2022. **211**: p. 118382.
  27. Yan, G., et al., Energy and exergy analysis of a new ejector enhanced auto-cascade refrigeration cycle. 2015. **105**: p. 509-517.
  28. Saleh, B.J.J.o.a.r., Parametric and working fluid analysis of a combined organic Rankine-vapor compression refrigeration system activated by low-grade thermal energy. 2016. **7**(5): p. 651-660.
  29. Wang, N., et al., Thermodynamic performance analysis a power and cooling generation system based on geothermal flash, organic Rankine cycles, and ejector refrigeration cycle; application of zeotropic mixtures. *Sustainable Energy Technologies and Assessments*, 2020. **40**: p. 100749.
  30. Elakhdar, M., et al., A combined thermal system of ejector refrigeration and Organic Rankine cycles for power generation using a solar parabolic trough. *Energy Conversion and Management*, 2019. **199**: p. 111947.
  31. Zheng, B. and Y.J.S.E. Weng, A combined power and ejector refrigeration cycle for low temperature heat sources. 2010. **84**(5): p. 784-791.
  32. Cao, Y., et al., Advanced exergy assessment of a solar absorption power cycle. *Renewable Energy*, 2022. **183**: p. 561-574.
  33. Rostamzadeh, H., et al., Exergoeconomic optimisation of basic and regenerative triple-evaporator combined power and refrigeration cycles. 2018. **26**(1-2): p. 186-225.
  34. Rostamzadeh, H., et al., Energy and exergy analysis of novel combined cooling and power (CCP) cycles. *Applied Thermal Engineering*, 2017. **124**: p. 152-169.
  35. Bejan, A., G. Tsatsaronis, and M.J. Moran, *Thermal design and optimization*. 1995: John Wiley & Sons.
  36. Ebadollahi, M., et al., Flexibility concept in design of advanced multi-energy carrier systems driven by biogas fuel for sustainable development. *Sustainable Cities and Society*, 2022. **86**: p. 104121.
  37. Ebadollahi, M., et al., Development of a novel flexible multigeneration energy system for meeting the energy needs of remote areas. *Renewable Energy*, 2022. **198**: p. 1224-1242.
  38. Safarian, S. and F.J.E.r. Aramoun, Energy and exergy assessments of modified Organic Rankine Cycles (ORCs). 2015. **1**: p. 1-7.